

8-2007

Pursuit-Evasion with Acceleration, Sensing Limitation, and Electronic Counter Measures

Jing-en Pang

Clemson University, jingenpang@hotmail.com

Follow this and additional works at: https://tigerprints.clemson.edu/all_theses



Part of the [Electrical and Computer Engineering Commons](#)

Recommended Citation

Pang, Jing-en, "Pursuit-Evasion with Acceleration, Sensing Limitation, and Electronic Counter Measures" (2007). *All Theses*. 164.
https://tigerprints.clemson.edu/all_theses/164

This Thesis is brought to you for free and open access by the Theses at TigerPrints. It has been accepted for inclusion in All Theses by an authorized administrator of TigerPrints. For more information, please contact kokeefe@clemson.edu.

PURSUIT-EVASION WITH ACCELERATION, SENSING LIMITATION, AND
ELECTRONIC COUNTER MEASURES

A Thesis
Presented to
the Graduate School of
Clemson University

In Partial Fulfillment
of the Requirements for the Degree
Master of Science
Electrical Engineering

by
Jing-En Pang
August 2007

Accepted by:
Richard Brooks, Committee Chair
Ian Walker
Adam Hoover

ABSTRACT

The use of game theory to analyze the optimal behaviors of both pursuers and evaders originated with Isaac's work at the Rand Corporation in the 1950's. Although many variations of this problem have been considered, published work to date is limited to the case where both players have constant velocities. In this thesis, we extend previous work by allowing players to accelerate. Analysis of this new problem using Newton's laws imposes an additional constraint to the system, which is the relationship between players' velocities and allowed turning radius. We find that analysis of this relationship provides new insight into the evader capture criteria for the constant velocity case. We summarize our results in a flow chart that expresses the parameter values that determine both the games of kind and games of degree associated with this problem. Pursuit-evasion games in the literature typically either assume both players have perfect knowledge of the opponent's position, or use primitive sensing models. These unrealistically skew the problem in favor of the pursuer who need only maintain a faster velocity at all turning radii. In real life, an evader usually escapes when the pursuer no longer knows the evader's position. We analyze the pursuit-evasion problem using a realistic sensor model and information theory to compute game theoretic payoff matrices. Our results show that this problem can be modeled as a two-person bi-matrix game. This game has a saddle point when the evader uses strategies that exploit sensor limitations, while the pursuer relies on strategies that ignore sensing limitations. Later we consider for the first time the effect of many types of electronic counter measures (ECM) on pursuit evasion games. The evader's decision to initiate its ECM is modeled as a function

of the distance between the players. Simulations show how to find optimal strategies for ECM use when initial conditions are known. We also discuss the effectiveness of different ECM technologies in pursuit-evasion games.

Keywords: Pursuit-Evasion, game theory, information theory, Electronic Counter Measures.

ACKNOWLEDGMENTS

First, I would like to thank my family who provides me the opportunity to study in US. Without them, I would not be where I am today.

Second, I wish to thank Dr. Brooks for motivating me, and providing me with support and guidance during the past two years. And I would also like to thank Dr. Walker and Dr. Hoover for taking the time from their busy schedules to review my thesis. Your effort is greatly appreciated.

Third, I would like to thank all my friends for their constant support and always being there for me.

This material is based upon work supported by, or in part by, the U. S. Army Research Laboratory and the U. S. Army Research Office under contract/grant number W911NF-05-1-0226.

TABLE OF CONTENTS

	Page
TITLE PAGE	i
ABSTRACT	ii
ACKNOWLEDGMENTS	iv
LIST OF TABLES	vii
LIST OF FIGURES	viii
CHAPTER	
I. INTRODUCTION	1
II. PURSUIT-EVASION BACKGROUND AND RELATED RESEARCH	5
III. MODELS FROM PHYSICS AND MATHEMATICS	8
3.1 Vehicle Dynamics	8
3.2 Finding an Optimal Path to a Point on the Plane	10
3.3 Finding the Maximum Region for a Vehicle	22
3.4 Finding the Approximate Front Boundary	26
IV. PURSUIT-EVASION WITH ACCELERATION	30
V. PURSUIT-EVASION WITH SENSING LIMITATION	38
5.1 Sensor Models	38
5.2 Information Theory Based Utility Function	41
5.3 Strategy for Games with Perfect Information	51
5.4 Experimental Results	52
VI. PURSUIT-EVASION WITH ELECTRONIC COUNTER MEASURES ..	57
6.1 Effect of Electronic Counter Measures	57
6.2 Experimental Results	58
VII. CONCLUSION AND FUTURE RESEARCH	67

Table of Contents (Continued)

	Page
APPENDICES	73
A: Circle Involute Background.....	74
B: Analysis of Non-Critical Path Optimal Paths	75
REFERENCES	77

LIST OF TABLES

Table		Page
5.1	Four possible outcomes of the target detection random process	38
5.2	Mean, variance, standard deviation, upper and lower 95% confident interval bounds for P 's ability to capture E in four different scenarios	55
5.3	Capture rate for each combination of strategy with different initial conditions	56

LIST OF FIGURES

Figure		Page
1.1	The vehicle cannot turn into the circular region defined by its minimum turning radius (MTR).....	1
3.1	Geometry of the vehicle dynamics in the absolute (world) coordinate system.....	10
3.2	Geometry of critical path of the vehicle with velocity not less than v_s	13
3.3	The vehicle reaches a point W above $I-Q-Q_1$ from point I through T_0 (case 1).....	15
3.4	The vehicle reaches a point W between $Q-Q_1$ and $Q-Q_2$ from point I (case 2).....	17
3.5	The vehicle reaches a point W between <i>Circle</i> (M, R_m) and $I-Q-Q_2$ (case 3)	19
3.6	The circle involute describes the curve traced by a string of a given length when wrapped onto a circle. When the vehicle velocity is less than v_s its motion is constrained only by its minimum turning radius R_m , and the curve describing the region $MR(t)$ when t is less than T_s is defined by a circle involute. This gives the maximum region for the vehicle until it reaches v_s	23
3.7	Until time T_s , region $MR(t)$ is defined by the circle involute. After T_s to reach points above the line tangent to the minimum turning radius circle at the point where it intersects the circle involute, the vehicle simply moves in a straight line.....	24
3.8	The maximum region the vehicle can reach by time T	25
3.9	The geometry of circle involute for pursuer or evader	26
3.10	The geometry of the initial condition of pursuit-evasion game	28

List of Figures (Continued)

Figure	Page
3.11 Curves show the possible positions at time t for pursuer (Blue, bottom) and evader (Red, right), both starting from the positions shown by crosses at time 0. The dotted line is Blue's effective sensing range	29
4.1 P 's capture region (solid) covers E 's escape region (dash). P captures E	36
4.2 P 's capture region (solid) doesn't cover E 's escape region (dash). E escapes.....	36
5.1 Classification of radar readings	42
5.2 P entropy strategy vs. E entropy strategy. Left: P found E ; Right: P lost E	53
5.3 P entropy strategy vs. E perfect sensor strategy. Left: P found E ; Right: P lost E	53
5.4 P perfect sensor strategy vs. E entropy strategy. Left: P found E ; Right: P lost E	54
5.5 P and E both perfect sensor strategy. P found E	54
6.1 Results for the first simulation using the nominal FP rate.....	60
6.2 Results for the second simulation using the nominal TP rate.....	60
6.3 Simulation results for representative combinations of TP and FP rates	61
6.4 Geometry explains why starting distance 85 has significant low capture rate.....	65
6.5 Simulation results for ECM where P and E use perfect information strategies.....	66
7.1 A flow chart that summarizes the games of kind for pursuit-evasion games with acceleration	68

List of Figures (Continued)

Figure	Page
A-1 The circle involute (bold curve) is formed by taking a line segment of a fixed length and wrapping it around a circle of a fixed radius. Angle $\theta = \angle IOM$, Line $IO = R$	74
B-1 Use different acceleration to reach tangent point T and go straight to point W	75

CHAPTER ONE

INTRODUCTION

Consider the problem of one vehicle attempting to overtake and capture a vehicle belonging to an opponent. In addition to being the central element of many Hollywood movie scripts, this problem has many practical applications, for example in the law enforcement and military domains. This problem is commonly known as a pursuit-evasion game; recent surveys of related research are in [1] and [26].

Pursuit-evasion games were originally posed in the 1950's as the "Homicidal Chauffeur Problem" in a series of Rand technical reports [9]. In that version of the problem, a slow pedestrian evader E , that can change direction at will, attempts to avoid being run over by a fast car driven by a homicidal pursuer P . E and P travel with constant speeds v_e and v_p , respectively. P 's minimum turning radius, i.e. the tightest turn possible for the vehicle due to its steering mechanism (see Figure 1.1), is R_{pm} .

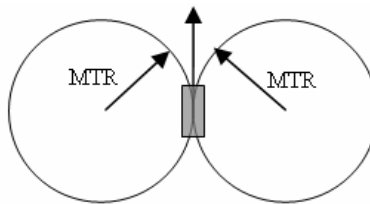


Figure 1.1: The vehicle cannot turn into the circular region defined by its minimum turning radius.

Depending on $\gamma = v_e/v_p < 1$, P captures E when:

$$1/R_{pm} > \sqrt{1-\gamma^2} + \sin^{-1} \gamma - 1 \tag{1.1}$$

If this inequality is reversed, E escapes from P [9].

In 1967, Cockayne [6] derived two necessary and sufficient conditions for P to be able to capture E . Using the notation introduced in this chapter, the conditions are:

$$v_p > v_e, \text{ and} \tag{1.2}$$

$$v_p^2 / R_{pm} \geq v_e^2 / R_{em} \tag{1.3}$$

Note that when velocities are constant and the terrain uniform, if capture is possible, with enough time it is asymptotically certain.

Analyses of pursuit-evasion games typically assume the pursuer has a faster velocity and the evader has a smaller minimum turning radius. But these models are not easily applied to most realistic situations, since they assume the velocities of both players are constant. This ignores the fact that each vehicle's ability to maneuver evasively during pursuit is largely constrained by its ability to accelerate and/or decelerate. In addition, as anyone who has driven an automobile can attest to, the maximum safe speed a vehicle can maintain is a function of its turning radius.

In this thesis, we start with the variant of the pursuit evasion game: a pursuer in an automobile tries to capture an intelligent evader in an automobile where both vehicles have limited acceleration and turning ability [2]. In this work, we find the conditions that determine the games of kind (the solution is a winning strategy for one of the players) but not the games of degree (the solution is a continuous value, ex. time to capture). This work also shows how the results of our analysis provide a new insight into the physical meaning of the capture criteria given in [6].

In this thesis, we modified this problem by having the pursuer and the evader both rely on sensors to determine the location of their opponents [3]. In that context, the

evader escapes when the pursuer no longer has actionable information about the evader's current position. Our sensor model considers the decay of the target's signature over distance. The sensor detection process in the model also has type I (false negative) and type II (false positive) errors. Information theoretic analysis of the sensor model provides a utility function that the evader uses to find its optimal escape strategy. Simulations confirmed that, by considering the pursuer's sensing limitations, the evader can greatly enhance its ability to escape.

In this thesis, we allow the evader to use Electronic Counter Measures (ECM) to modify the true positive and false positive error rates of the pursuer's radar. In modern combat, electronic counter measures play an important role in this process. A number of electronic counter measures exist where one participant can intentionally disrupt the sensing capability of their opponent. Common countermeasure technologies include:

- ◆ Chaff – used to trigger a large number of false positives.
- ◆ Aerosols – used to attenuate signals and lower the true positive rate.
- ◆ Deception and blip enhancement – modifies the readings returned by a sensor to skew readings, increase their variance, or modify target classification.
- ◆ Flares and decoys – mimic target signatures to produce multiple tracks, only one of which belongs to the real target.

The rest of this thesis is organized as follows: Chapter Two reviews previous pursuit-evasion game researches; In Chapter Three, a review of vehicle dynamics, critical path, maximum region, and front boundary are provided; Chapter Four explains our pursuit-evasion game with acceleration; Chapter Five explains our pursuit-evasion game

with sensor; Chapter Six explains our pursuit-evasion game with electronic counter measures; Chapter Seven gives conclusions and describes areas for future research.

CHAPTER TWO

PURSUIT-EVASION BACKGROUND AND RELATED RESEARCH

In this Chapter we review related pursuit-evasion games that have been presented in the literature. The pursuit-evasion problem was originally called the “Homicidal Chauffeur Problem” in [9]. A more agile but slower evader E tries to avoid being run over by a faster pursuer P . P 's motion is constrained by a minimum turning radius R . E has no minimum turning radius and can change direction at will. A more symmetric variant of this problem, where both P and E drive cars with fixed speeds and respective turning radii R_{pm} and R_{em} , is presented in Merz's 1971 PhD dissertation [20]. He fully solved the games of kind and degree¹ for this problem [21]. He also considered the problem of finding which player, given specific initial conditions, is better positioned to be the pursuer [23]. This analysis is very useful for determining aerial combat strategies as shown in [22] and [14]. Vehicles that move in 3-dimensions have six degrees of freedom. In addition to movement in the x , y , and z directions, there are the following degrees of freedom related to their orientation: pitch, roll and yaw. If we consider a vehicle centered coordinate system where the y -axis is the vehicle's longitudinal (from tail to nose) axis, the x -axis is the horizontal perpendicular to the y -axis (parallel to the wings), and the z -axis is perpendicular to the xy plane. Then, the vehicle pitch is rotation about the x -axis, roll is rotation about the y -axis and yaw is rotation about the z -axis. Most conventional aircraft and high speed missiles have limited yaw rates and therefore

¹ A game of kind is a qualitative game with a fixed set of outcomes; typically the outcome is simply which player wins. A game of degree is a quantitative game that has an infinite number of possible outcomes, e.g. the time to capture.

perform bank-to-turn maneuvers to avoid using the yaw degree of freedom. The results in [24] use this insight to show how the 3-D problem reduces to the 2-D problem for these classes of aircraft. They show how to calculate critical values for the difference between the roll rates of the pursuer and evader. If the pursuer's roll rate is not sufficiently larger than the evader's, then the evader will escape. If the pursuer's roll rate is sufficiently greater, the pursuer has optimal maneuvers that allow it to constrain the evader to maneuvers within the same xy plane. In which case, as long as it is safe to assume that the maximum allowable velocities for the vehicles are limited by the centrifugal force that they experience, then our results should hold for 3-D problems as well. Note that our results should apply to combat aircraft where maneuverability is limited by the amount of force the pilot can sustain without losing consciousness.

One recent pursuit-evasion variant is the "herding dog and sheep problem," in which one dog attempts to steer many sheep to a given location. The deterministic case of this problem can be solved using dynamic programming [12]. A stochastic variant is considered in [13]. That work extends the pursuit-evasion problem by allowing multiple evaders, but it doesn't consider some real world factors such as varying speed, turning radius, vehicle rollover, acceleration, etc. Many on many games are considered in [31]. A team of unmanned aerial and ground vehicles pursues a team of evaders in an unknown terrain. They integrate autonomous agents with heterogeneous capabilities into an intelligent adaptive system and propose a distributed hierarchical hybrid system architecture that emphasizes the autonomy of each agent and allows for coordinated team efforts.

Very little work has been done on pursuit evasion problems with imperfect information. Some researchers have considered pursuit-evasion games in classes of terrains where the pursuer's field of view is limited. A path-planning algorithm in [16] guarantees that all evaders will eventually be detected in an environment with occlusions defined by arbitrary curves. This extends the work in [15]. Occluded visions in polygonal environments were considered in [10]. In that work, randomized pursuer strategies were analyzed. The only ECM related pursuit evasion research to our knowledge is Ph.D. dissertation [17] where the evader uses decoys to confuse the pursuer. To the best of our knowledge this is the first research to consider the classes of ECM problems that we have used.

CHAPTER THREE

MODELS FROM PHYSICS AND MATHEMATICS

3.1 Vehicle Dynamics

In our game, the pursuing vehicle P chases the evading vehicle E . Both vehicles follow Newton's laws for circular motion along a circle of radius R , where R is limited from below by R_{pm} and R_{em} , respectively, as in Figure 1.1.

Our approach determines the nominal path that a vehicle should follow during a pursuit-evasion game. Many problems with real vehicle motion, such as wheel slippage, are not explicitly expressed in these equations. Wheel slippage is outside the scope of this thesis, since it is a reaction to an unforeseen event and not something that affects the vehicle's pursuit-evasion strategy. It would be trivial to extend our approach to handle slippage and related issues, by using our solutions as a nominal control signal for a drive-by-wire feedback controller, like the one in [31] that senses the vehicle's interactions with its environment.

Another problem with vehicle motion is roll over. As a vehicle turns, a centripetal force is generated on its center of mass. This force in turn generates a torque that may cause the vehicle to rollover. The strength of this torque is easily predicted using Newton's second law. The centripetal force on a vehicle with mass M moving with turning radius R and velocity v has magnitude $F_{roll} = M v^2/R$. The vehicle will roll over if the centripetal force exceeds a threshold value F_{roll} that depends on its suspension and design. The vehicle will remain stable when $v^2/R \leq F_{roll}/M$. Since F_{roll} and M are properties of the vehicle, this constraint becomes:

$$v^2/R \leq K_{roll} = F_{roll}/M \quad (3.1)$$

Note that factor K_{roll} adds physical insight to the capture condition from Cockayne [6]; vehicles able to turn at higher velocities have an advantage. From Equation (3.1), we derive the vehicle's safe velocity v_s . A vehicle traveling at a velocity slower than v_s can turn with any turning radius greater than or equal to its minimum turning radius. If the minimum turning radius is R_m and the maximum velocity is v_m , then:

$$v_s = \min(v_m, \sqrt{K_{roll} \cdot R_m}) \quad (3.2)$$

We also derive the safe turning radius R_s . The vehicle can travel at any velocity less than its maximum velocity with the turning radius greater than or equal to R_s , i.e.:

$$R_s = \max(R_m, v_m^2/K_{roll}) \quad (3.3)$$

Given the current velocity v_c , we derive the current allowed minimum turning radius R_c . The vehicle can turn with any turning radius greater than or equal to its R_c , i.e.:

$$R_c = \max(R_m, v_c^2/K_{roll}) \quad (3.4)$$

Each player has two control variables, $u(t)$ and $a(t)$. The use of control variable $u(t)$, where $u(t) = R_c/R(t)$, is described in [9]. The vehicle travels on a circle of radius $R(t) = R_c/u(t)$, where $u(t)$ ranges from -1 to 1. This lets the player choose the instantaneous turning radius and also allows the vehicle to move in a straight line (i.e. $u(t) = 0$), without explicitly dealing with an infinite turning radius. The other control variable, $a(t)$, is the instantaneous acceleration at any point in time, which is bounded from above by a vehicle dependent maximum acceleration constant, a_m . The instantaneous vehicle velocity, which is also bounded from above by a vehicle dependent constant, can be

calculated at any point in time from the vehicle's initial velocity and the history of $a(t)$ values. These equations of motion from [5] express Newton's equations for circular motion with acceleration in terms of the two control variables (see Figure 3.1):

$$\begin{aligned}
 \dot{x}(t) &= v_c(t) \cdot \sin \varphi(t) \\
 \dot{y}(t) &= v_c(t) \cdot \cos \varphi(t) \\
 \dot{\varphi}(t) &= v_c(t) \cdot u(t) / R_c(t) \\
 R_c(t) &= \max(R_m, v_c^2(t) / K_{roll}) \\
 v_c(t) &= v_0 + \int_0^t a(\tau) \cdot d\tau
 \end{aligned} \tag{3.5}$$

where x and y represent the position with respect to $(0, 0)$; φ represents the vehicles orientation with respect to Y -axis; v_0 is the initial velocity and K_{roll} is the rollover constant .

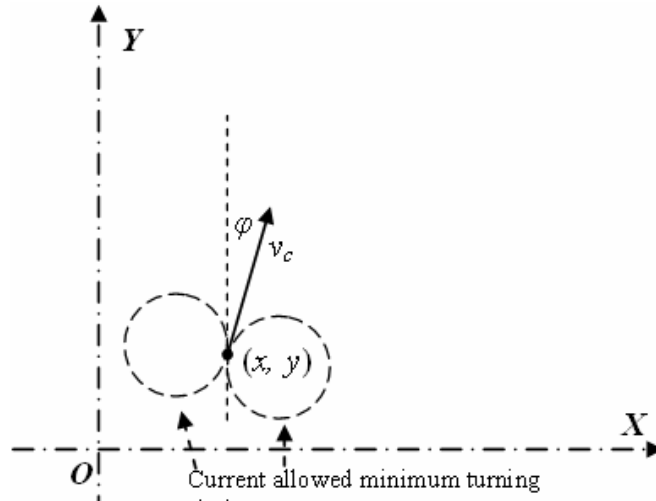


Figure 3.1: Geometry of the vehicle dynamics in the absolute (world) coordinate system.

3.2 Finding an Optimal Path to a Point on the Plane

In this chapter, we define the *optimal path* to any point W in the plane as the path that takes the vehicle from its initial position to W in the minimal amount of time. If the

vehicle can reach W without turning, that path is a straight line and its ability to reach W is limited only by its maximum velocity and acceleration. If W is on the current allowed minimum turning circle with radius R_c defined by Equation (3.4), the optimal path is an arc on that circle.

If W is inside the vehicle's current allowed minimum turning circle defined by R_c , it is temporarily unreachable. The optimal path to these points is more difficult to determine, since the vehicle must reach a position where W is outside that circle (see [9] for a detailed analysis of this problem with the homicidal chauffeur constraints). For the rest of this Chapter, we discuss only paths to points to the right of the vehicle. Equivalent paths for points to the left can be found by symmetry.

For some points, finding the optimal path is straightforward. Let v_0 be the initial velocity. If $v_0 < v_s$ (Equation (3.2)), until the vehicle reaches v_s it can accelerate with the maximum rate a_m and turn with any turning radius greater than or equal to R_m . For any point W outside the turning circle with radius R_m , there is a line tangent to the circle that passes through W . The vehicle travels first along the minimum turning circle. If the vehicle reaches the point where the tangent line intersects the circle before it reaches v_s , the optimal path follows the circle with radius R_m to the tangent line and then follows the tangent line to W . While on this path, the vehicle accelerates with a_m until it reaches v_m . Once it reaches v_m , the vehicle must stop accelerating. This path is clearly optimal, since it is the shortest distance the vehicle can follow between the two points and the vehicle is moving as quickly as possible at all points on the path. There is a region in front of the vehicle that contains all these points.

The rest of Chapter 3 explains how to find the boundaries of regions containing points whose optimal paths are found using similar methods. By finding the paths that are boundaries between regions, we determine how to find the optimal path to any given point.

Since the optimal path from any initial position to the point where the vehicle reaches v_s is clearly defined, we ignore this path segment for the rest of the discussion and assume that the vehicle starts from a position with velocity $v_0 \geq v_s$. We also express circles as “*Circle (center, radius)*” for the rest of the discussion.

If the vehicle reaches v_s before reaching the tangent point on its minimum turning circle, from that point on the turning radius and velocity are mutually constrained by Equation (3.1). From Equation (3.4), given an instantaneous velocity v_c , the allowed minimum turning radius is $R_c = v_c^2/K_{roll} \geq R_m$. We now consider the path where the vehicle accelerates with a_m (until reaching v_m) while turning as tightly as possible (i.e., $u(t)=1$) without rolling over.

In Figure 3.2, the vehicle starts at point I with initial velocity $v_0 = v_s$ directed along the arrow. It turns around *Circle*(M, R_m). Its velocity increases with $v_c(t) = v_0 + a_m t$, during which the allowed minimum turning radius increases as $v_c(t)^2/K_{roll}$. This continues until the vehicle reaches v_m at point Q . The vehicle can then go straight following the tangent line $Q-Q_1$ or continue turning along the circle with radius R_s (Equation (3.3)) following arc $Q-Q_2$.

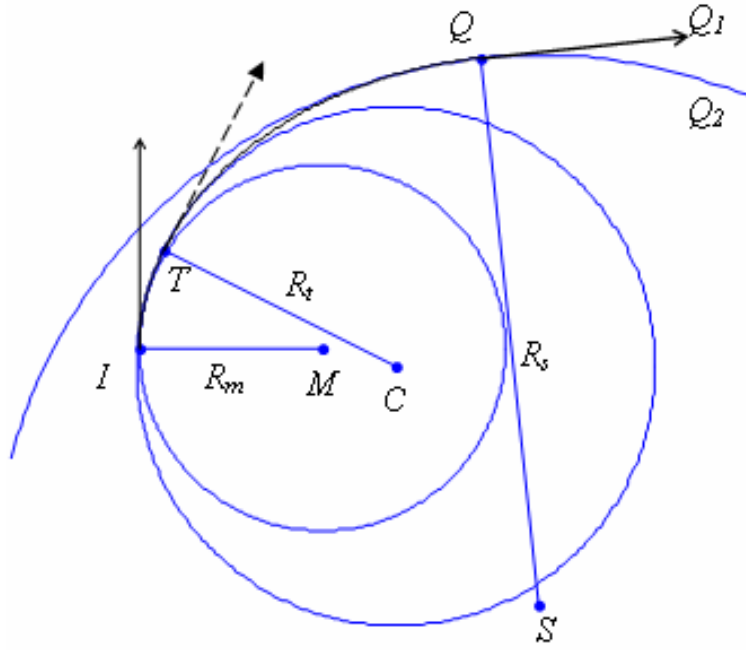


Figure 3.2: Geometry of critical path of the vehicle with velocity not less than v_s .

Path $I-Q-Q_1$ is the *Critical Path*. The minimum turning circle is $Circle(M, R_m)$ and the safe turning circle is $Circle(S, R_s)$. For any point T on path IQ , when the vehicle is at T it has velocity v_t and allowed turning circle, $Circle(C, R_t)$. For each point T on path IQ , the vehicle has position $(x(t), y(t))$ and orientation $\varphi(t)$ giving:

$$\begin{aligned}
 \dot{x}(t) &= v_c(t) \sin(\varphi(t)) \\
 \dot{y}(t) &= v_c(t) \cos(\varphi(t)) \\
 \dot{\varphi}(t) &= v_c(t) / R_c(t) \\
 v_c(t) &= v_0 + a_m t \\
 v_c^2(t) / R_c(t) &= K \\
 0 \leq t &\leq (v_m - v_0) / a_m, \quad v_s \leq v_0 \leq v_m \\
 x(0) = y(0) = \varphi(0) &= 0.
 \end{aligned} \tag{3.6}$$

We solve these equations by:

$$\begin{aligned}\dot{\varphi}(t) &= v_c(t)/R_c(t), \quad v_c(t) = v_0 + a_m \cdot t, \quad v_c^2(t)/R_c(t) = K_{roll} \\ \Rightarrow \dot{\varphi}(t) &= \frac{K_{roll}}{v_0 + a_m t} \Rightarrow \varphi(t) = \int_0^t \frac{K_{roll}}{v_0 + a_m t} dt = \frac{K}{a_m} (\log(v_0 + a_m t) - \log(v_0))\end{aligned}$$

$$\dot{x}(t) = (v_0 + a_m t) \cdot \sin\left(\frac{K_{roll}}{a_m} (\log(v_0 + a_m t) - \log(v_0))\right)$$

$$\dot{y}(t) = (v_0 + a_m t) \cdot \cos\left(\frac{K_{roll}}{a_m} (\log(v_0 + a_m t) - \log(v_0))\right)$$

$$\text{Let } \log(v_0 + a_m t) = r, \quad K_{roll}/a_m = c, \quad K_{roll} \cdot \log(v_0)/a_m = d.$$

$$\text{Then } \dot{x}(t) = e^{2r} \cdot \sin(cr - d)/a_m$$

$$\Rightarrow x(t) = \int e^r \cdot \sin(cr - d) dr = e^r \sin(cr - d) - c \int e^r \cos(cr - d) dr$$

$$= e^r \sin(cr - d) - c(e^r \cos(cr - d) + c \int e^r \sin(cr - d) dr)$$

$$\Rightarrow (1 + c^2) \cdot \int e^r \cdot \sin(cr - d) dr = e^r \cdot \sin(cr - d) - c \cdot e^r \cos(cr - d)$$

$$\Rightarrow x(t) = \frac{2e^{2r} \cdot \sin(cr - d) - c \cdot e^{2r} \cos(cr - d)}{a_m(c^2 + 4)}$$

By substituting variables and applying the same method to $y(t)$, we get:

$$\varphi(t) = \frac{K_{roll}}{a_m} (\log(v_0 + a_m t) - \log(v_0))$$

$$x(t) = \frac{(v_0 + a_m t)^2}{4a_m^2 + K_{roll}^2} [2a_m \sin(\varphi(t)) - K_{roll} \cos(\varphi(t))] + \frac{K_{roll} v_0^2}{4a_m^2 + K_{roll}^2} \quad (3.7)$$

$$y(t) = \frac{(v_0 + a_m t)^2}{4a_m^2 + K_{roll}^2} [2a_m \cos(\varphi(t)) + K_{roll} \sin(\varphi(t))] - \frac{2a_m v_0^2}{4a_m^2 + K_{roll}^2}$$

$$\text{given } 0 \leq t \leq (v_m - v_0)/a_m, \quad v_s \leq v_0 \leq v_m.$$

Since the initial velocity v_0 is greater than or equal to v_s , $R_t = v_0^2/K_{roll}$. The vehicle starts at point T (see Figure 3.2), with its heading given by the dotted arrow. The path from I (or T) to point Q is uniquely defined by Equation (3.7). Point Q_1 is a distant point on the tangent line of this path at point Q (where the vehicle reaches v_m).

Another path $I-Q-Q_2$ occurs when the vehicle continues turning with $u(t)=1$ from Q . It turns with radius R_s towards point Q_2 . We now separate the problem into three distinct cases: 1) points “above” $I-Q-Q_1$ (i.e. point W , Figure 3.3), 2) points between $Q-Q_1$ and $Q-Q_2$ (Figure 3.4), and 3) points “below” $I-Q-Q_2$ and outside $Circle(M, R_m)$ (Figure 3.5). The rest of our discussion only considers the path after the vehicle reaches velocity v_s , since the path to that point is already uniquely defined. For that reason, without loss of generality, we will say that the initial velocity is greater than or equal to v_s .

3.2.1 Case 1

Theorem 3.1: The optimal path for point W above path $I-Q-Q_1$ lies between paths $I-T_0-W$ and $I-T_m-W$.

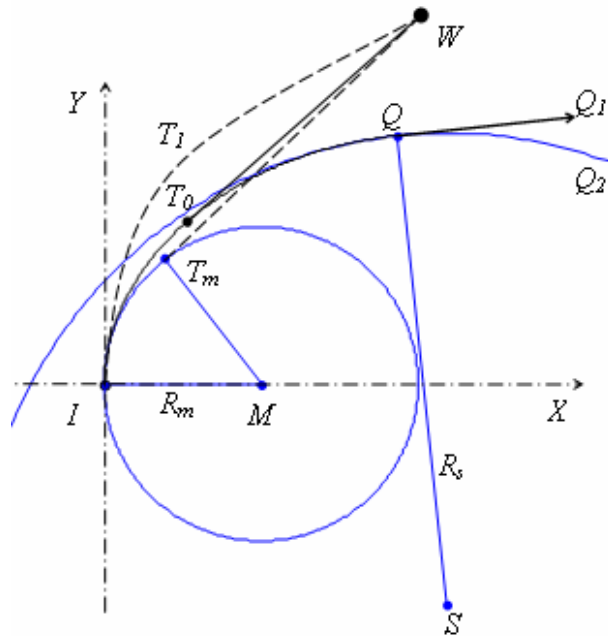


Figure 3.3: The vehicle reaches a point W above $I-Q-Q_1$ from point I through T_0 (case 1).

Proof: Suppose the vehicle starts at point $I(0, 0)$ oriented towards Y , and its goal is point W located above $I-Q-Q_1$ as in Figure 3.3. One way for the vehicle to reach W is to travel along $I-Q-Q_1$ until reaching tangent point T_0 and then take the tangent line straight to W . On path $I-T_0-W$ the vehicle accelerates with a_m until it reaches v_m , it then travels with v_m . It is not possible for it to move more quickly along any other path. When compared to any path $I-T_1-W$ above it, path $I-T_0-W$ is shorter and therefore quicker. So the optimal path can not lie above $I-T_0-W$.

Alternatively, the vehicle can travel along minimum turning circle $Circle(M, R_m)$ to point T_m where it intersects its tangent line to W . The vehicle then follows the tangent line straight to W . This path $I-T_m-W$ is the shortest possible path to W . Any path below $I-T_m-W$ will take longer to reach W , since it cannot accelerate more quickly and must travel a greater distance. The optimal path, which reaches W in the shortest time, must therefore lie between $I-T_0-W$ and $I-T_m-W$. (QED)

The path $I-T_0-W$ has the higher velocity and $I-T_m-W$ has the shorter length. We note from Figure 3.3 that these paths are very similar. Using trigonometry we see that as the distance to W grows, the size of this difference shrinks asymptotically. Since the vehicle accelerates more quickly along $I-T_0-W$ it has a higher velocity, so eventually path $I-T_0-W$ will become optimal. It is the optimal path for almost every point in this region.

There may be a small set of points between paths $I-T_m-W$ and $I-T_0-W$ where $I-T_0-W$ is not optimal. In Appendix B we describe how to find the optimal path numerically

for this set of points. In practice, we advise ignoring the results of Appendix B and simply following the critical path. This is based on the following insights:

- ◆ The distance between paths $I-T_m-W$ and $I-T_0-W$ is almost always inconsequential, so that any improvement from using the truly optimal path is likely to be minimal.
- ◆ The time required to calculate this path numerically is almost certain to be greater than the performance improvement attained.

3.2.2 Case 2

Theorem 3.2: For any point W between paths $Q-Q_1$ and $Q-Q_2$, the optimal path from I to W is $I-T_0-Q'-W$.

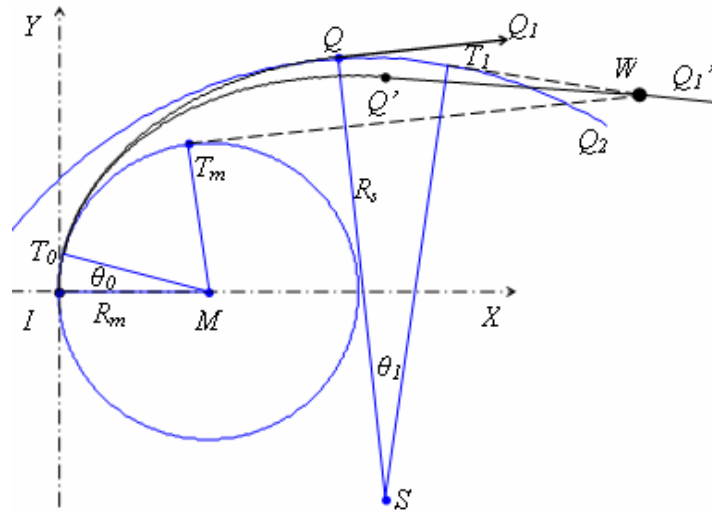


Figure 3.4: The vehicle reaches a point W between $Q-Q_1$ and $Q-Q_2$ from point I (case 2).

Proof: In this case (Figure 3.4) the vehicle's goal point W is located between line $Q-Q_1$ and curve $Q-Q_2$. We start our analysis by finding the point T_0 on $Circle(M, R_m)$ that is the

first point that can correspond to point I in Figure 3.3. Path $T_0-Q'-Q_1'$ is the critical path from T_0 , where T_0 and Q' correspond to I and Q in Case 1. W must now lie on line $Q'-Q_1'$. One way to reach W is to travel along $Circle(M, R_m)$ to T_0 ; and then accelerate with a_m and set $u(t)=1$. This is like traveling along the critical path. The vehicle passes Q' where it reaches v_m and then goes straight to W , following path $I-T_0-Q'-W$.

An alternative path to W takes critical path $I-Q$ to $Circle(S, R_s)$, which it follows to point T_1 where the tangent line to W intersects $Circle(S, R_s)$. The vehicle then takes the tangent line straight to W . This is path $I-Q-T_1-W$ in Figure 3.4.

Let's define $\theta_0 = \text{Angle}(IMT_0)$ and $\theta_1 = \text{Angle}(QST_1)$. In path $I-T_0-Q'-W$, the vehicle turns along $Circle(M, R_m)$ for θ_0 degrees and then travels the critical path. In path $I-Q-T_1-W$, the vehicle travels the critical path and then along $Circle(S, R_s)$ for θ_1 degrees. Using trigonometry, we see that $\theta_1 = \theta_0$. The time difference between these two paths is due to the time spent traveling on the two circles.

The time traveling θ_0 along $Circle(M, R_m)$ is $t_1 = R_m\theta_0 / v_s$. The time traveling θ_1 along $Circle(S, R_s)$ is $t_2 = R_s\theta_1 / v_m$. Since $v_m^2/R_s = v_s^2/R_m$ and $v_m > v_s$, we have $v_m/R_s < v_s/R_m$ or $R_s / v_m > R_m / v_s$, i.e. $t_1 < t_2$. Path $I-T_0-Q'-W$ is therefore always faster than path $I-Q-T_1-W$. The same argument holds for all paths between the two paths. The vehicle should therefore never travel above path $I-T_0-Q'-W$.

A third path travels along $Circle(M, R_m)$ to point T_m where the circle intersects its tangent line to W . It then follows the tangent line straight to W . This is path $I-T_m-W$ in Figure 3.4. This is the shortest possible path to W . Any path beneath this must travel further at a lower velocity. Path $I-T_0-Q'-W$ and path $I-T_m-W$ are identical until T_0 .

From case 1, we know that path $T_0-Q'-W$ is better than any path between $T_0-Q'-W$ and T_0-T_m-W . This demonstrates that the optimal path can not lie beneath path $I-T_0-Q'-W$. This proves that path $I-T_0-Q'-W$ is the optimal path to any point W between $Q-Q_1$ and $Q-Q_2$. (QED)

3.2.3 Case 3

Theorem 3.3: Path $I-T_0-cp-W$ is the time optimal path from points I to W in Figure 3.5.

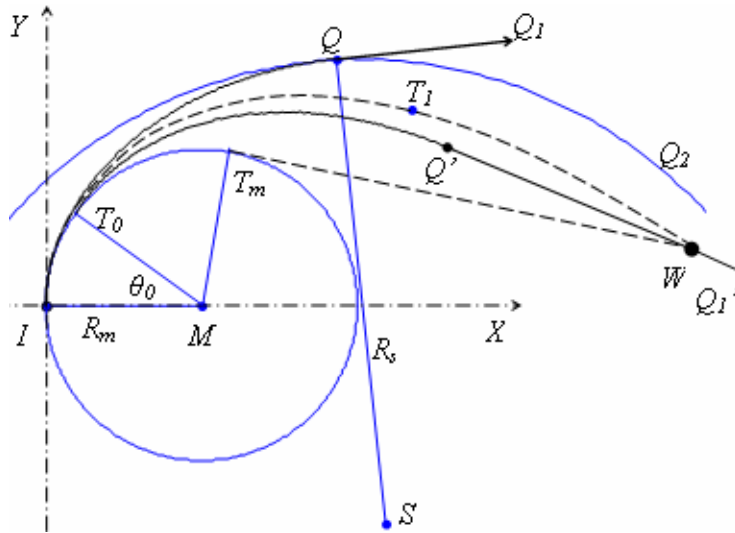


Figure 3.5: The vehicle reaches a point W between $Circle(M, R_m)$ and $I-Q-Q_2$ (case 3).

Proof: In this case (see Figure 3.5) the vehicle's goal point W is located between $Circle(M, R_m)$ and path $I-Q-Q_2$. (Note that games involving points inside $Circle(M, R_m)$ are handled in detail in [9].) As with case 2, we find point T_0 on $Circle(M, R_m)$ that is the earliest point with a critical path of the form $T_0-Q'-Q_1'$ that reaches W . Using the same logic as in case 2, W must lie on path $T_0-Q'-Q_1'$. If W is on curve T_0-Q' , the vehicle will not be traveling with velocity v_m at W . If W is on line $Q'-Q_1'$, it will have velocity v_m at W .

One way to reach W is path $I-T_0\text{-}cp\text{-}W$, which follows $Circle(M, R_m)$ to T_0 and then follows the critical path to W . As with cases 1 and 2 any path above $I-T_0\text{-}cp\text{-}W$ will be suboptimal, since the path will be longer than $I-T_0\text{-}cp\text{-}W$ and the vehicle can not be moving with a larger velocity at any point in time.

We now draw a tangent line from W that intersects $Circle(M, R_m)$ at T_m and consider path $I-T_0\text{-}T_m\text{-}W$. Using the same logic as in case 2, any path beneath $I-T_0\text{-}T_m\text{-}W$ will require more time than $I-T_0\text{-}T_m\text{-}W$ and any path between $I-T_0\text{-}T_m\text{-}W$ (including $I-T_0\text{-}T_m\text{-}W$) and $I-T_0\text{-}cp\text{-}W$ will require more time than path $I-T_0\text{-}cp\text{-}W$.

Path $I-T_0\text{-}cp\text{-}W$ must therefore be the optimal path to any point W between $Circle(M, R_m)$ and $I-Q-Q_2$ from I . (QED)

3.2.4 The General Case

From almost all initial conditions, the shortest time path from an initial starting position to a given point in the plane can be found following the same general procedure. The two exceptions being:

- ◆ Points inside the minimum turning circle require complicated maneuvers. We do not treat this problem here, as it is handled in depth in [9]. To reach these points, the pursuer maneuvers to a position where the point is no longer in its minimum turning circle. Without loss of generality, we can perform the analysis given in this Chapter at the end of the maneuver suggested in [9].
- ◆ Some goal points from Case 1 are reached more quickly using a path between $I-T_1\text{-}W$ and $I-T_0\text{-}W$. These exceptions are discussed in depth in Chapter 3.2.1.

For all other cases, given any initial velocity v_0 and an arbitrary goal point on the plane, if v_0 is less than v_s , accelerate with a_m until the velocity is v_s or v_m and turn with $u(t)$ being 1 or -1 until one of the following occurs:

- ◆ If the tangent line is reached, take the tangent line directly to W .
- ◆ When v is greater than or equal to v_s , find the instantaneous critical path. If the point is above the critical path, accelerate with a_m until v is v_m and turn as much as possible (i.e. $u=1$ or -1) until the line tangent to W is reached, then follow the line to W .
- ◆ If the point is below the critical path, use the current velocity to turn along the current minimum turning circle ($a=0$, $u=1$ or -1). When W is on the vehicle's critical path, follow the critical path to W ($a=a_m$ before v_m , $a=0$ after v_m ; $u=1$ or -1 before the tangent line, $u=0$ after).

Note that the vehicle always sets its control values to some combination of $a = 0$ or a_m and $u = 0, 1, \text{ or } -1$. This can be visualized using an elastic string and a spool. The string will follow the constraining spool (i.e. $u(t)=1$) until there is a straight line to its other end (i.e. $u(t)=0$). The elastic string naturally conforms to the shortest path between its ends to minimize the tension. For the acceleration, if the vehicle needs to hug the currently allowed minimum turning circle, it sets a to 0; otherwise, it accelerates using the maximum acceleration a_m as long as it can.²

² This behavior could have been predicted by noting that the characteristics of Equation (3.5) indicate the Hamiltonian corresponding to the minimum time problem has a degenerate critical point in the controls. That is, the control is expected to be "bang-bang." This derivation is not used since it requires more complex mathematics and omits all intuition gained in our preceding discussion.

3.3 Finding the Maximum Region for a Vehicle

This chapter shows how to find the maximum region $MR(t)$, the region containing all points the vehicle can reach by time t starting from the initial conditions. Alternatively, this could be considered the smallest region guaranteed to contain a vehicle at time t that started from a known initial position at time t_0 .

The vehicle starts at point $O(0, 0)$ with velocity $v_0 \leq v_m$. If the vehicle travels in a straight line, it may accelerate for at most $t_a = \min(T, (v_m - v_0)/a_m)$ time units. Therefore, the longest distance d it can travel by time T is:

$$d(T) = v_0 t_a + a_m t_a^2 / 2 + v_m (T - t_a). \quad (3.8)$$

If v_0 is less than v_s , the vehicle requires time $T_s = (v_s - v_0)/a_m$ to reach v_s . As long as the current velocity $v(t)$ is less than v_s , the vehicle can turn with any turning radius greater than the minimum turning radius R_m . To find $MR(t)$ for any time t less than T_s , we first calculate $d(T_s)$. We then find $MR(t)$ by cutting a string of length $d(T_s)$, attaching one end of the string to the vehicle's initial position, and tracing the curve defined by the other end of the taut string as it moves from the constraining circle defined by R_m on the left to the constraining circle defined by R_m on the right. This curve is the involute of a circle of radius R_m (see Appendix A for details). The circle involute together with the minimum turning circles defines the maximum region for the vehicle up until it reaches v_s . The point O is the initial position (see Figure 3.6). The two dashed circles are the minimum turning circles $Circle(M, R_m)$ and $Circle(M', R_m)$. The solid curves indicate the front boundary of the maximum region at different values of t . The bold solid curve is the *safe-*

velocity curve, which indicates when the vehicle reaches v_s and intersects the minimum turning circle at point S on the right, S' on the left.

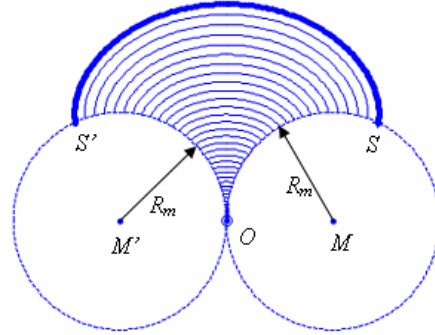


Figure 3.6: The circle involute describes the curve traced by a string of a given length when wrapped onto a circle. When the vehicle velocity is less than v_s its motion is constrained only by its minimum turning radius R_m , and the curve describing the region $MR(t)$ when t is less than T_s is defined by a circle involute. This gives the maximum region for the vehicle until it reaches v_s .

Once the vehicle reaches velocity v_s , two cases exist. The rest of our discussion considers the right half of the region; results for the left half can be found using symmetry. Our two cases are separated by a line tangent to $Circle(M, R_m)$ at the point S , where the involute intersects the circle.

3.3.1 Case 1

This is the region above the tangent line. The vehicle accelerates until it reaches v_s and then continues moving in a straight line. Its motion is not constrained by the factor K_{roll} defined in Equation (3.1).

To find the maximum region for this case, calculate the maximum straight distance d that the vehicle can travel. Cut a string with length d and attach one end on O

and using the taut string to wrap $\text{Circle}(M, R_m)$ until it touches S . The track of another end of the string is the front boundary of the max region above the tangent line, which is a circle involute. The upper part of the region, shown in Figure 3.7, is defined by this curve and the tangent lines.

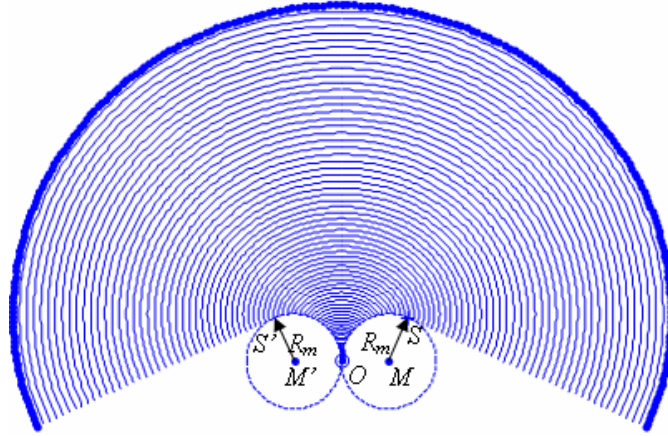


Figure 3.7: Until time T_s , region $MR(t)$ is defined by the circle involute. After T_s to reach points above the line tangent to the minimum turning radius circle at the point where it intersects the circle involute, the vehicle simply moves in a straight line.

3.3.2 Case 2

Below the tangent line, the vehicle's ability to turn is limited by its velocity (Equation (3.3)). Recall the optimal path defined in Chapter 3.2. In Chapter 3.2.4, we show that a vehicle reaches a given point in the shortest time by following the critical path as soon as it exists.

By using relative coordinates centered on the vehicle when it reaches point S , we map this problem to the one shown in Figure 3.2 with equivalent point I . This divides the region into two sub-cases: above and below path $I-Q-Q_1$. In the first sub-case, the vehicle travels along the critical path for time t_1 and then straight. By setting t_1 to $T - T_s$

(including zero), we find that the region above the critical path from point S is enclosed by the end points of these paths. In the second sub-case, in the remaining time $T - T_s$, the vehicle travels along $Circle(M, R_m)$ for time t_1 and then follows the critical path once it exists. By setting t_1 to $T - T_s$ (including zero), we find the set of points enclosing the part of the maximum region located below the critical path from point S .

By taking the union of these sub-cases with the results from case 1, we find the maximum region (see Figure 3.8) a vehicle can reach by time T .

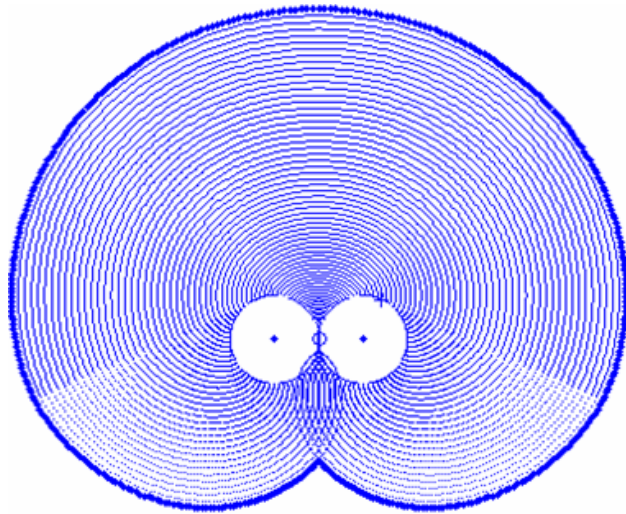


Figure 3.8: The maximum region the vehicle can reach by time T .

In Figure 3.8, we can see that points inside the left (right) minimum turning circle can be reached by traveling to the right (left) then going straight. Alternatively, the vehicle can go straight until the point is outside the instantaneous minimum turning circle then turn around.

3.4 Finding the Approximate Front Boundary

In this game, there is no discernable advantage to moving at less than the maximum velocity possible at any moment. Therefore, we assume in this thesis that each player uses the maximum acceleration possible (within constraints imposed by Equations (3.1) and (3.4)) at any point in time. This means that each player has only one control variable, $u(t)$ the rate of turn. We discuss this assumption further in the Conclusion Chapter. If the distance between pursuer and evader is far, the difference between turning with R_s and R_c (see Equation (3.2) and (3.3)) could be ignored. Therefore, in optimal play with perfect knowledge $u(t)$ is typically set to either 0 or values corresponding to R_s .

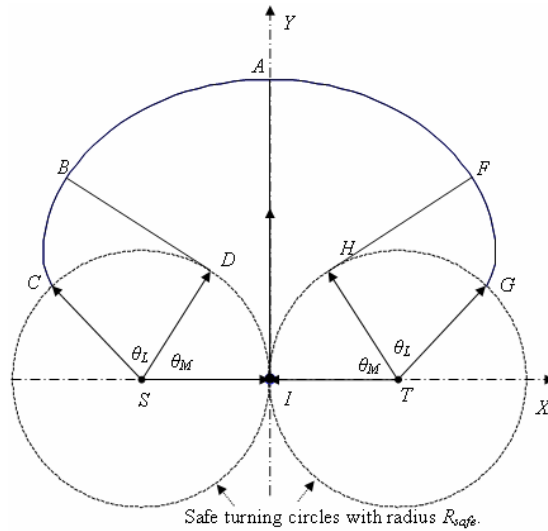


Figure 3.9: The geometry of circle involute for pursuer or evader.

In Figure 3.9, a player with initial position I is traveling along the Y axis. The dashed circles have radius R_s . Up to time t , the player can reach any point within region $IDCBAFGHI$. To reach that point, the player turns as quickly as possible for its current velocity until it reaches a specific angle then it follows a straight line. The derivation of

this optimal strategy is in [2]. We define the angle that the vehicle turns as θ_M (angle *DSI* or *HTI* in Figure 3.9). We refer to angles *CSD* and *GTH* as θ_L , and angles *CSI* and *GTI* as θ_H . Since we assume both players accelerate with their maximum acceleration, the player will be somewhere on arc *BAF* at any given time t . The player can go furthest by going straight, and we call this distance $travel(t)$ (line *IA* in Figure 3.9). Given current velocity v_c , maximum velocity v_m and maximum acceleration a_m , $travel(t)$ is calculated as:

$$\begin{aligned} T_a &= \min((v_m - v_c) / a_m, t), \\ travel(t) &= v_c T_a + a_m T_a^2 / 2 + v_m (t - T_a) \end{aligned} \quad (3.9)$$

If we center the XY coordinate system on point I , the equation for arc *BAF* is:

$$\begin{pmatrix} x(t) \\ y(t) \end{pmatrix} = \begin{pmatrix} \cos(\theta_H - \pi) & \sin(\theta_H - \pi) \\ -\sin(\theta_H - \pi) & \cos(\theta_H - \pi) \end{pmatrix} \begin{pmatrix} R_s (\cos \theta + \theta \cdot \sin \theta) \\ R_s (\sin \theta - \theta \cdot \cos \theta) \end{pmatrix} + \begin{pmatrix} R_s \\ 0 \end{pmatrix} \quad (3.10)$$

where $\theta_L \leq \theta \leq \theta_H$, $\theta_H = travel(t) / R_{safe}$, $\theta_L = \max(0, \theta_H - \theta_M)$.

The length of *BAF* is:

$$length = R_s (\theta_H^2 - \theta_L^2) \quad (3.11)$$

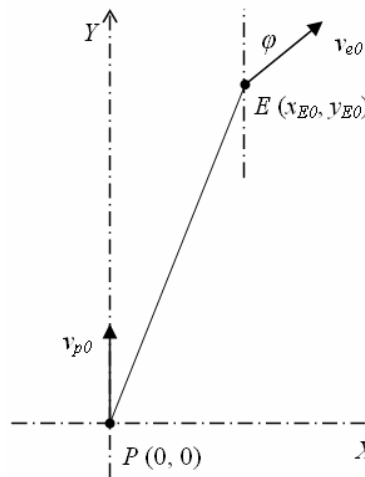


Figure 3.10: The geometry of the initial condition of pursuit-evasion game.

In our game, P initially has velocity v_{p0} at position $(0, 0)$ heading along the Y -axis. E initially has velocity v_{e0} at position (x_{E0}, y_{E0}) heading along angle φ with respect to the Y -axis, as shown in Figure 3.10.

We now express the positions for both players as a function of the safe turning radius, acceleration, initial position and time:

◆ For the pursuer:

$$\begin{pmatrix} x'_p(t) \\ y'_p(t) \end{pmatrix} = \begin{pmatrix} \cos(\theta_{PH} - \pi) & \sin(\theta_{PH} - \pi) \\ -\sin(\theta_{PH} - \pi) & \cos(\theta_{PH} - \pi) \end{pmatrix} \begin{pmatrix} R_{P.s}(\cos \theta_p + \theta_p \cdot \sin \theta_p) \\ R_{P.s}(\sin \theta_p - \theta_p \cdot \cos \theta_p) \end{pmatrix} + \begin{pmatrix} R_{P.s} \\ 0 \end{pmatrix}$$

where $\theta_p \in [\theta_{PL}, \theta_{PH}]$, $\theta_{PH} = \frac{\text{travel}_P(t)}{R_{P.s}}$, $\theta_{PL} = \max(0, \theta_{PH} - \theta_{PM})$

$$\begin{pmatrix} x_p(t) \\ y_p(t) \end{pmatrix} = \begin{pmatrix} \pm x'_p(t) \\ y'_p(t) \end{pmatrix} \quad (3.12)$$

◆ For the evader:

$$\begin{pmatrix} x'_e(t) \\ y'_e(t) \end{pmatrix} = \begin{pmatrix} \cos(\theta_{EH} - \pi) & \sin(\theta_{EH} - \pi) \\ -\sin(\theta_{EH} - \pi) & \cos(\theta_{EH} - \pi) \end{pmatrix} \begin{pmatrix} R_{E.s}(\cos \theta_e + \theta_e \cdot \sin \theta_e) \\ R_{E.s}(\sin \theta_e - \theta_e \cdot \cos \theta_e) \end{pmatrix} + \begin{pmatrix} R_{E.s} \\ 0 \end{pmatrix}$$

where $\theta_e \in [\theta_{EL}, \theta_{EH}]$, $\theta_{EH} = \frac{\text{travel}_E(t)}{R_{E.s}}$, $\theta_{EL} = \max(0, \theta_{EH} - \theta_{EM})$

$$\begin{pmatrix} x_e(t) \\ y_e(t) \end{pmatrix} = \begin{pmatrix} \cos \varphi & \sin \varphi \\ -\sin \varphi & \cos \varphi \end{pmatrix} \cdot \begin{pmatrix} \pm x'_e(t) \\ y'_e(t) \end{pmatrix} + \begin{pmatrix} x_{E0} \\ y_{E0} \end{pmatrix} \quad (3.13)$$

Equation (3.12) expresses the pursuer's BAF curve, which we call its front boundary. Equation (3.13) is the evader's front boundary, where φ is their relative direction and (x_{E0}, y_{E0}) is the relative initial position of the evader as shown in Figure 3.10. So at time t , the set of possible positions for each player is constrained to the solid boundary arcs shown in Figure 3.11.

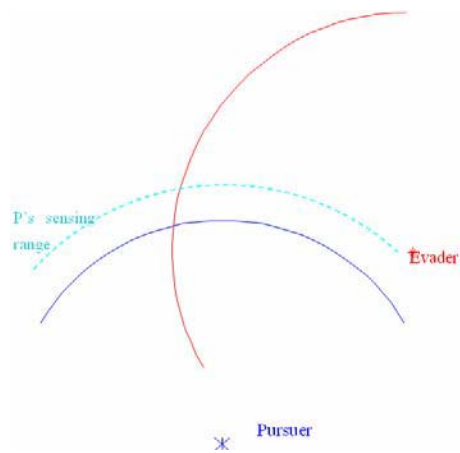


Figure 3.11: Curves show the possible positions at time t for pursuer (Blue, bottom) and evader (Red, right), both starting from the positions shown by crosses at time 0. The dotted line is Blue's effective sensing range.

For any given positions of pursuer and evader, the Euclidean distance between them is:

$$d_{PE}(t) = \sqrt{(x_E(t) - x_P(t))^2 + (y_E(t) - y_P(t))^2} \quad (3.14)$$

CHAPTER FOUR

PURSUIT-EVASION WITH ACCELERATION

Assume P (pursuer) and E (evader) move in the plane with constant speeds v_p and v_e , respectively. R_{pm} and R_{em} are their respective minimum turning radii. The following two conditions determine the game of kind:

$$\begin{aligned} A) \quad & v_p > v_e \\ B) \quad & v_p^2 / R_{pm} \geq v_e^2 / R_{em} \end{aligned} \quad (4.1)$$

Theorem 4.1: If and only if A) and B) are satisfied, P can capture E from any initial position. The proof of Theorem 4.1 can be found in [6].

Instead of assuming a constant velocity for both pursuer and evader, we use the vehicle dynamics presented in Equation (3.5) in Chapter 3.1. The players can accelerate until they reach maximum velocities. Their velocities and turning radii constrain each other. In Figure 3.10, the pursuer P and evader E is characterized by the following constants: maximum velocity v_{pm} and v_{em} , maximum acceleration a_{pm} and a_{em} , minimum turning radius R_{pm} and R_{em} and rollover coefficient $K_{p,roll}$ and $K_{e,roll}$, respectively. P initially has velocity v_{p0} at position $(0, 0)$ heading along the Y -axis. E initially has velocity v_{e0} at position (x_0, y_0) heading along angle φ with respect to the Y -axis.

Each vehicle's equations of motion are defined by the initial conditions and Equation (3.5). We now analyze the game using a relative coordinate system centered on P . If P is at point (x_p, y_p) heading in direction φ_p and E is at point (x_e, y_e) heading in

direction φ_e in the absolute coordinate system. We let (x_r, y_r) and φ_r be E 's position and heading in the relative coordinate system. This gives:

$$\begin{aligned}x_r &= (x_e - x_p)\cos\varphi_p - (y_e - y_p)\sin\varphi_p \\y_r &= (x_e - x_p)\sin\varphi_p + (y_e - y_p)\cos\varphi_p \\ \varphi_r &= \varphi_e - \varphi_p\end{aligned}\tag{4.2a}$$

$$\text{Or } \begin{pmatrix} x_r \\ y_r \\ \varphi_r \end{pmatrix} = \begin{pmatrix} \cos(\varphi_p) & -\sin(\varphi_p) & 0 \\ \sin(\varphi_p) & \cos(\varphi_p) & 0 \\ 0 & 0 & 1 \end{pmatrix} \begin{pmatrix} x_e - x_p \\ y_e - y_p \\ \varphi_e - \varphi_p \end{pmatrix}\tag{4.2b}$$

The system dynamics in the relative coordinate system becomes:

$$\begin{aligned}\dot{x}_r(t) &= -\frac{v_p(t)}{R_{pc}(t)}y_r(t)u_p(t) + v_e(t)\sin\varphi_r(t) \\ \dot{y}_r(t) &= \frac{v_p(t)}{R_{pc}(t)}x_r(t)u_p(t) - v_p(t) + v_e(t)\cos\varphi_r(t) \\ \dot{\varphi}_r(t) &= -v_p(t)\frac{u_p(t)}{R_{pc}(t)} + v_e(t)\frac{u_e(t)}{R_{ec}(t)}\end{aligned}\tag{4.3}$$

$$R_{pc}(t) = \max\left(R_{pm}, \frac{v_p^2(t)}{K_{p.roll}}\right)$$

$$R_{ec}(t) = \max\left(R_{em}, \frac{v_e^2(t)}{K_{e.roll}}\right)$$

$$v_p(t) = v_p(0) + \int_0^t a_p(\tau)d\tau$$

$$v_e(t) = v_e(0) + \int_0^t a_e(\tau)d\tau$$

$$\begin{cases} 0 \leq a_p(\tau) \leq a_{pm} & \text{if } v_p(\tau) < v_{pm} \\ a_p(\tau) = 0 & \text{if } v_p(\tau) = v_{pm} \end{cases}$$

$$\begin{cases} 0 \leq a_e(\tau) \leq a_{em} & \text{if } v_e(\tau) < v_{em} \\ a_e(\tau) = 0 & \text{if } v_e(\tau) = v_{em} \end{cases}$$

$$-1 \leq u_p(t), u_e(t) \leq 1$$

If the distance between both players is bounded from above, we say that the pursuer controls the evader. If at some time, the distance between P and E goes to zero, we say that the pursuer captures the evader. If the distance between the players is unbounded over time, we say that the evader escapes from the pursuer.

Let's consider this game using region $MR(t)$ from previous chapter. If $v_{pm} > v_{em}$, P 's region will eventually include E 's entire region. So that, for any set of initial conditions, P can always control E . But if $v_{pm} < v_{em}$, if the initial conditions are favorable, P can control E for a certain period of time and even capture E . We now determine the criteria of both capture and escape.

Theorem 4.2: If $K_p < K_e$, i.e. $v_p^2/R_p < v_e^2/R_e$, E can avoid capture by P .

Proof: Recall conditions A) and B) from [6] (see Equation (4.1)). Although, in contrast to [6], velocities are not constant in our game, each vehicle's motion is constrained by condition $v^2/R \leq K_{roll}$. As shown in Chapter 3.2, the optimal paths to points where velocity and turning radius require are mutually constrained require $v^2/R = K_{roll}$ for part of the path. At any point in time, the vehicles current velocity v_c limits the vehicle's effective minimum turning radius to $R_c \geq v_c^2/K_{roll}$. Substituting this inequality into condition B) we see that, since K_{roll} is a constant for each player, condition B) will either be uniformly true or false for any instance of our pursuit-evasion game. When $K_{p,roll} < K_{e,roll}$, condition B) does not hold. Thus P will not be able to capture E . (QED)

Theorem 4.3: If $K_{p,roll} \geq K_{e,roll}$ and $v_{pm} > v_{em}$, P captures E eventually.

Proof: We consider the game as time t approaches infinity. We have established that $K_{p.roll} \geq K_{e.roll}$ corresponds to condition B) from Theorem 4.1. If the pursuer has a larger maximum velocity, no matter what the initial conditions, eventually $v_p(t) > v_e(t)$. Then condition A) is satisfied. Now since both conditions of Theorem 4.1 are satisfied. We conclude that P can capture E . (QED)

For the rest of this chapter, we consider the case where the pursuer has a larger rollover coefficient but smaller maximum velocity than the evader, i.e. $K_{p.roll} \geq K_{e.roll}$ and $v_{pm} < v_{em}$. Under these conditions, we need to account for the vehicles' initial velocities, v_{p0} , v_{e0} , and maximum acceleration, a_{pm} , a_{em} . For P to capture E , it must have a higher velocity than E for some period of time. For E to escape from P , it needs only reach v_{pm} before capture. Without loss of generalization, we assume that P 's acceleration is greater than E 's if P 's maximum velocity is less than E 's.

Since the capture conditions for both players depend on which has the higher velocity, there is no reason for them to ever use less than the maximum acceleration until they reach their maximum allowed velocities, i.e.:

$$\begin{aligned}
 a_p &= \begin{cases} a_{pm} & \text{if } v_p < v_{pm} \text{ and accelerate} \\ 0 & \text{otherwise} \end{cases} \\
 a_e &= \begin{cases} a_{em} & \text{if } v_e < v_{em} \text{ and accelerate} \\ 0 & \text{otherwise} \end{cases} \\
 a_{pm} &> a_{em}, \quad v_{pm} < v_{em} \text{ (by current assumption)}
 \end{aligned} \tag{4.4}$$

The following times are critical to our analysis: T_e is minimum time for E reaches its maximum velocity, T_p is minimum time for P reaches its maximum velocity, and T_{ed} is minimum time for E reaches the P 's maximum velocity.

$$T_e = \frac{v_{em} - v_{e0}}{a_{em}}; \quad T_p = \frac{v_{pm} - v_{p0}}{a_{pm}}; \quad T_{ed} = \frac{v_{pm} - v_{e0}}{a_{em}} \quad (4.5)$$

Lemma 4.1: Assuming $a_{pm} > a_{em}$, $v_{pm} < v_{em}$, and $T_{ed} < T_p$. Let $v_e(t) = \min(v_{e0} + a_{em}t, v_{em})$, and $v_p(t) = \min(v_{p0} + a_{pm}t, v_{pm})$. Then $v_e(t) > v_p(t)$ for all t .

Proof: Let $F(t) = v_e(t) - v_p(t)$. When $t > T_{ed}$, by definition, E will have velocity greater than v_{pm} , which is the max velocity of P . Then $F(t) > 0$ and $v_e(t) > v_p(t)$. Consider $t \leq T_{ed}$. Since $a_{pm} > a_{em}$, $v_{pm} < v_{em}$, $T_{ed} < T_p$, it is easy to show $v_{e0} > v_{p0}$, i.e. $v_e(0) > v_p(0)$, and $v_e(T_{ed}) > v_p(T_{ed})$. Since $a_{pm} > a_{em}$, $F(t)$ is continuous and non-increasing. By mean value theorem, it follows that $F(t) > 0$. (QED)

Theorem 4.4: Given $K_{p.roll} \geq K_{e.roll}$, $v_{pm} < v_{em}$, $a_{pm} > a_{em}$, E can escape from P if $(v_{pm} - v_{p0})/a_{pm} > (v_{pm} - v_{e0})/a_{em}$, i.e. $T_p > T_{ed}$.

Proof: If $T_{ed} < T_p$, by Lemma 4.1, E will always have velocity greater than P . Condition A) is never satisfied. We conclude that P can never capture E . Since E has a higher velocity, the distance between them is unbounded and P cannot control E . E escapes from P . (QED)

When $T_{ed} > T_p$, and P has a higher velocity than E for some period of time. Let the earliest time when P has a higher velocity be t_1 . From $v_{p0} + a_{pm}t_1 > v_{e0} + a_{em}t_1$, we have $t_1 = (v_{e0} - v_{p0}) / (a_{pm} - a_{em})$. If $v_{e0} < v_{p0}$, P has higher initial velocity, i.e. $t_1 = 0$. So, $t_1 = \max(0, (v_{e0} - v_{p0}) / (a_{pm} - a_{em}))$.

Let P have a higher velocity no later than t_2 . E can then turn with its current allowed minimum turning radius and then accelerate until it reaches P 's maximum velocity. $R_{ec} = \max(R_{em}, v_{e0}^2/K_{e.roll})$, $t_2 = 2\pi R_{ec}/v_{e0} + (v_{pm} - v_{e0})/a_{em}$.

P 's capture region, denoted by $PCR(t)$, is calculated by finding the maximum region between t_1 and t_2 .

E 's escape region, denoted by $EER(t)$ is calculated by: 1) Calculate the boundary of E 's maximum region from time $t = t_1$. 2) Retain the region which is not in $PCR(t)$; Compute the front boundary in discrete points and calculate the maximum region for time $t = t_1 + dt$ from the these points.³ Repeat 2) until time $t = t_2$. The union of the regions kept in 2) is E 's escape region.

Theorem 4.5: Given $K_{p.roll} \geq K_{e.roll}$, $v_{pm} < v_{em}$, $a_{pm} > a_{em}$ and $(v_{pm} - v_{p0})/a_{pm} < (v_{pm} - v_{e0})/a_{em}$, we can find the time period from t_1 to t_2 , when $v_e < v_p$: $t_1 = \max\{0, (v_{e0} - v_{p0}) / (a_{pm} - a_{em})\}$ and $R_{ec} = \max(R_{em}, v_{e0}^2/K_{e.roll})$, $t_2 = 2\pi R_{ec}/v_{e0} + (v_{pm} - v_{e0})/a_{em}$. Using the optimal path to find the capture region for P and the maximum escape region for E , if P 's region covers E 's, P can capture E .

Proof: If P 's region covers E 's region, since P has a higher velocity and higher rollover constant, condition A) and B) are satisfied, i.e. P captures E , shown in Figure 4.1.

Otherwise, that means E has a path to go out of P 's control and can violate condition A).

So E escapes from P , shown in Figure 4.2. (QED)

³ This is simply a numerical integration using a first order approximation. Improved approximations can be obtained using higher order methods. In our experience, this approach is sufficient.

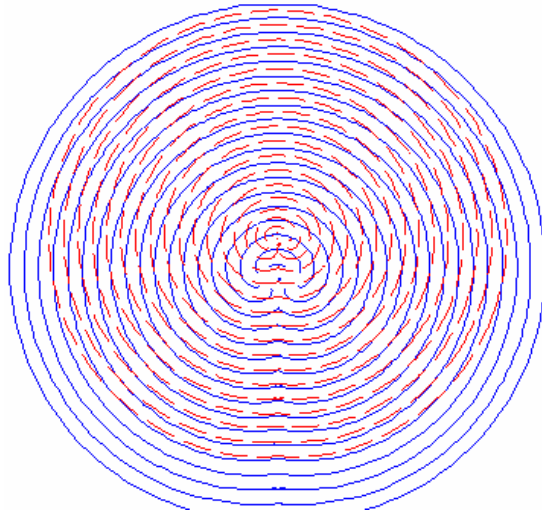


Figure 4.1: P 's capture region (solid) covers E 's escape region (dash). P captures E .

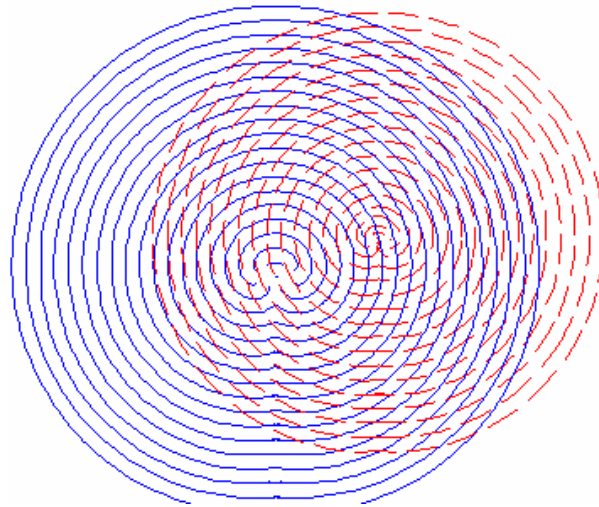


Figure 4.2: P 's capture region (solid) doesn't cover E 's escape region (dash). E escapes.

The cases where $K_{p,roll} \geq K_{e,roll}$, $v_{pm} < v_{em}$ and $a_{pm} < a_{em}$, can be solved in a similar manner. If P has a lower initial velocity, E can escape. If P has a higher initial velocity, $R_{ec} = \max(R_{em}, v_{e0}^2 / K_{e,roll})$, $t_2 = 2\pi R_{ec} / v_{e0} + (v_{pm} - v_{e0}) / a_{em}$.

It is straightforward to apply these results to solving the game of degree for this problem. If E can escape then the value of the game is infinite and E 's strategy is to take

any trajectory that remains outside of P 's capture region. If E can not escape from P , but is not controlled by P , then the value of the game is infinite and E 's strategy is to evade P in the final stages of capture. In both cases P 's strategy is irrelevant, since it is doomed to failure.

If E can not escape and is controlled by P , then the value of the game is the time when P 's capture region first envelopes E 's escape region. E 's optimal strategy is to follow the optimal path to any of the points that are on the intersection of the boundary's of both regions at that time. P 's optimal strategy is to choose a path that asymptotically converges with the observed path of E .

CHAPTER FIVE

PURSUIT-EVASION WITH SENSING LIMITATIONS

5.1 Sensor Model

Pursuit evasion research to date has concentrated either on systems with perfect knowledge, or with sensors whose sole limitation is a geometric range constraint. In real life, the ability of a sensor to detect an object is subject to an array of environmental influences and noise sources that make sensor range unpredictable at best [11, 32]. For military applications, sensor readings can also be subject to electronic counter measures (ECM) that are designed to modify sensor inputs in ways that deceive the detection process.

	Target present	Target absent
Target detected	TP: True Positive	FP: False Positive (Type II error)
Target not detected	FN: False Negative (Type I error)	TN: True Negative

Table 5.1: Four possible outcomes of the target detection random process

Instead of using a cookie cutter model [32], we consider sensing to be the process of detecting a known target signature obscured by background noise. For a given sensor input, this process outputs one of the four outcomes in Table 5.1. TP is true positive, the target is detected and present; FP is false positive, the target is detected but absent (Type II error); FN is false negative, the target is present but not detected (Type I error); And

TN is true negative, the target is absent and not detected. For TP and TN, the sensor works correctly. FN (FP) corresponds to Type I (Type II) error in decision theory.

The sensor target (pursuer or evader) emits a signal in a noisy environment. The sensor must differentiate between the target signal and random background noise. When the target signal is weak, its spectrum is hidden in the noise. Typically, the sensor detects a target only when the target signal's power exceeds a fixed threshold. Receiver Operating Characteristics (ROC) curves are used to find the optimal threshold as described in [32].

For signals subject to Gaussian noise and propagating in a homogeneous medium, the signal strength, and therefore probability of detection, decays as an inverse exponential of the distance d between the sensor and the target. This gives probability of detection:

$$P(TP) = Cd^{-\alpha} \quad (5.1)$$

where α varies in practice from 2 to 5 [36]. Note that probability should be bounded between 0 and 1. And $P(TP)$ is already greater than zero but may exceed one, so in fact, $P(TP) = \min(1, Cd^{-\alpha})$. In the following of this thesis, when we mention $Cd^{-\alpha}$, for easy representation, it means $\min(1, Cd^{-\alpha})$. In this thesis, we use $\alpha = 4$, which corresponds to the radar equation [32]. Since the false alarm rate is dependent solely on background noise, we make the common assumption of a constant false alarm rate, i.e. $P(FP) = K_{FP} = \text{constant}$. This assumption is tenable as long as the background noise is uncorrelated, which is the case in a homogeneous environment. Using Table 5.1 and the fact that when

a target is present it is either detected or not detected, we get $P(\text{FN}) = 1 - P(\text{TP})$. Similarly, an absent target is either detected or not, giving $P(\text{TN}) = 1 - P(\text{FP})$.

We note in passing that, although the Gaussian signal decay in free space assumption is ubiquitous in signal processing, it does not always correspond to reality. Occlusion, signal shadowing, multi-path fading, scattering, and clutter are often responsible for signal decay that does not follow Equation (5.1). A fuller discussion of those issues, along with a theoretical approach that allows derivation of more realistic hit rates $P(\text{TP})$ and distributions can be found in [34, 35]. For the sake of simplicity, we use Equation (5.1) in the examples given here. The concepts in [34, 35] can be used to generalize these results to more complex cluttered environments.

We use decision theory to decide, given a sensor reading, whether the reading is correct or in error. Therefore, we conclude that a target is present only when $P(\text{TP}) > P(\text{FP})$. The effective sensing range of our sensor is therefore R_{sense} where $CR_{\text{sense}}^{-\alpha} = P(\text{FP})$, i.e.:

$$R_{\text{sense}} = (P(\text{FP})/C)^{\alpha} \quad (5.2)$$

If no *a priori* evidence is available, we believe that detections within (outside) this range are true positives (false alarms) simply because this is the most probable case.

The signal attenuation factor is typically in the range $2 \leq \alpha \leq 5$ [36] depending on the sensing modality. Of particular interest are the following cases:

- ◆ $\alpha = 2$ for acoustic and seismic sensing. The signal propagates in a plane. Its power dissipates proportional to the area of a circle centered on the signal source.
- ◆ $\alpha = 3$ for image or video sensors [32]. Detection rate is tied to target size in the

image, which shrinks with d^3 . For signals propagating in a 3-dimensional space power will dissipate proportional to the volume of a sphere centered on the source.

- ◆ $\alpha = 4$ for radar detection, since it corresponds to the radar equation [32]. Radar is an active sensor. The signal dissipates on its way to the target from the sensor and while returning to the sensor. We use $\alpha = 4$ in our examples in this thesis.

5.2 Information Theory Based Utility Function

We consider pursuit evasion games like the ones summarized in Chapter 4 and handled in detail in [2]. The only difference is that in this chapter the pursuer and evader rely on sensors to get information about each other's position. Since this is a pursuit game and not a search game [29], we assume both the pursuer and evader start with *a priori* information regarding each other's position.

In a game with perfect information it does not matter how far the evader gets from the pursuer or how often it evades capture, the pursuer always knows where the evader is. The evader can never elude the pursuer; it can only out run the pursuer. An evader with a faster maximum velocity will evade capture even when the pursuer has perfect information and does not need to exploit the pursuer's sensing weaknesses to win. Similarly, to exploit sensing weaknesses, the evader will need to be able to reach a region where the pursuer's sensing capability is weak. For these reasons, we assume in this game that the pursuer has a larger maximum velocity but the evader has a larger maximum acceleration and initial velocity. We also assume that the distance between the

two is large enough for the evader to temporarily move outside the pursuer's radar's effective sensing range.

We assume that the pursuer and evader have perfect *a priori* information of each other's positions at the beginning of the game. But after that time, both players rely on their sensor inputs. A sensor reading is a tuple consisting of time, detection state and target coordinates (when a target is detected). When a false positive occurs, the sensor returns random coordinates within the effective sensing range. As shown in Figure 5.1, at any point in time the pursuer's radar has two possible states: target detected or no target detected. If there is a detection, the pursuer needs to decide whether the detection is a true positive (TP) or false positive (FP). This classification is done by determining which case is most likely, given the *a priori* information. When no target is detected (ND), the system needs to determine whether the reading is a true negative (TN) or false negative (FN), again using *a priori* information. A no detection event is a true negative if the evader is outside the radar's effective sensing range, as defined in Equation (5.2) in Chapter 5.

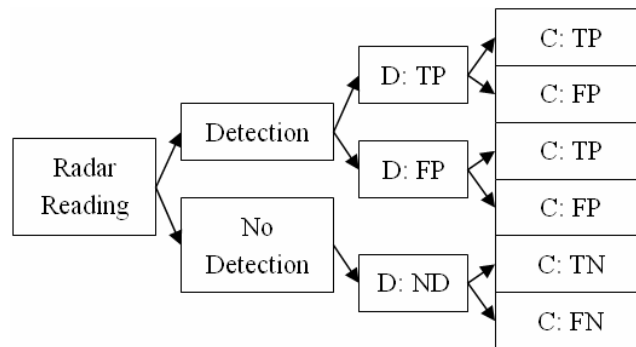


Figure 5.1: Classification of radar readings.

Figure 5.1 illustrates the classification process. There are three detection states: TP, FP, and ND and for each state the system can classify it as either true or false. In Figure 5.1 “D” refers to the sensor reading and “C” refers to the player’s interpretation (classification) of the sensor reading. A detection event classification can refer to one of four possible combinations: true positive classified as true positive (TP TP), true positive classified as false positive (TP FP), false positive classified as false positive (FP FP) or false positive classified as true positive (FP TP). However, no detection only has two possible belief classifications: (ND TN) or (ND FN). We explain the reason for this distinction later in this chapter. We denote the six blocks on the right to be cases 1 through 6. Their associated probabilities are $p_1, p_2 \dots p_6$.

Since the P and E each start with *a priori* knowledge of each other’s location, they are aware that the future positions both players may have at time t are constrained to the boundary curves in Figure 3.11. Since both vehicles move with the maximum allowable velocity, their strategy is defined purely by the turning rate $u(t)$. This means that for pursuer P and evader E each strategy corresponds to a point on their boundary curve, and for each combination of P and E strategies the distance d between the two vehicles is easily computed. We now derive a payoff matrix where each element (i, j) of the matrix corresponds to the amount of certainty that P will have about E ’s position if P uses strategy i (corresponding to a discrete point of P ’s boundary curve) and E uses position j (corresponding to a discrete point of E ’s boundary curve). This is done by:

- ◆ Calculating the distance d between P and E ’s positions,
- ◆ Calculating the likelihood p_k of each of the cases presented in Figure 6,

- ◆ Calculating the *a posteriori* belief function pdf_k that P would have about E 's location as a result of the sensor returns for the associated case,
- ◆ Using the entropy e_{ij} of $\sum_k p_k pdf_k$ to express the amount of disorder in P 's *a posteriori* belief function, and
- ◆ Setting the payoff matrix element (i, j) value to the expected strength s_{ij} of E 's target signature should both players pursue strategy (i, j) minus e_{ij} .

5.2.1 Probabilities of cases

We now show how to determine the probabilities of each of the six cases in Figure 5.1 occurring for any combination of strategies for both players. When the opponent is at distance d , the likelihood that the player's radar will detect the opponent (TP) is probability Cd^α , and the likelihood that the radar returns a false positive (FP) is K_{FP} . Both C and K_{FP} are constants, and d is the distance between the radar and the target. The probability of no detection (ND) is $P(\text{ND}) = 1 - (Cd^\alpha + K_{FP})$. Note that FP and TP always have a non-zero probability, regardless of the target's position. When an ND occurs, it is a true negative (TN) when the target is located outside the effective sensing range. The ND is a false negative (FN) when the target is located inside the effective sensing range. Therefore, at any time in the game there are always two possible detection events (TP or FP) and only one possible no detection event (ND). This is why we have six cases and not eight cases.

The evader will be located on its boundary curve within a width sigma σ_r , that we use to account for movement uncertainty. The area of this region is $A_1 = length_r * \sigma_r$, where $length_r$ is twice of length in Equation (3.11). We denote the area of the sensing range as $A_2 = \pi * R_{sense}^2$. We denote the likelihood that a false positive reading occurs within area A_1 as A_1/A_2 .

We now consider true positive detections ($D=TP$). Based on the true positive and false positive probabilities, if $Cd^\alpha > K_{FP} A_1/A_2$, we conclude it to be a true positive ($C=TP$). Otherwise, we conclude that it is a false positive ($C=FP$), since that is more likely. If the detection is false positive ($D=FP$), our conclusion will be the same as ($D=TP$). Consider the cases where the radar does not detect a target: true negative (TN) and false negative (FN). The probability of non-detection is $1 - \text{Prob}(\text{detection}) = 1 - Cd^\alpha - K_{FP}$. When the target is outside the effective sensing range and we do not detect it, it is a TN. When the target is inside the effective sensing range but we don't detect it, it is a FN. The classification decision is based on the sensing range. Since the likelihood of a non-detection event is $(1 - Cd^\alpha - K_{FP})$, and the only variable in the equation is d , this decision amounts to deciding whether it is more likely that the non-detection is associated with values of d greater than the effective sensing range or less than the effective sensing range. Since d^α decreases as d increases, the TN decision is the more likely interpretation as long as the *a priori* information allows this possibility. So we have the following probabilities for the 6 cases to occur at a given moment:

$$\begin{aligned}
p_1 &= \text{prob}(D = TP \ \& \ C = TP) = \text{prob}(Cd^{-\alpha} > K_{FP}A_1 / A_2) \cdot Cd^{-\alpha} \\
p_2 &= \text{prob}(D = TP \ \& \ C = FP) = \text{prob}(Cd^{-\alpha} < K_{FP}A_1 / A_2) \cdot Cd^{-\alpha} \\
p_3 &= \text{prob}(D = FP \ \& \ C = TP) = \text{prob}(Cd^{-\alpha} > K_{FP}A_1 / A_2) \cdot K_{FP} \\
p_4 &= \text{prob}(D = FP \ \& \ C = FP) = \text{prob}(Cd^{-\alpha} < K_{FP}A_1 / A_2) \cdot K_{FP} \\
p_5 &= \text{prob}(D = ND \ \& \ C = TN) = (1 - Cd^{-\alpha} - K_{FP}) \ \& \ \text{part of boundary arc outside } R_{sense} \\
p_6 &= \text{prob}(D = ND \ \& \ C = FN) = (1 - Cd^{-\alpha} - K_{FP}) \ \& \ \text{whole boundary arc within } R_{sense}
\end{aligned} \tag{5.3}$$

Note that these probabilities are solely dependent on the distance between P and E , and that the first term in the *RHS* of Equations (5.3) can be calculated geometrically as the proportion of the domain where the Boolean statement is true.

5.2.2 *a posteriori* belief functions

Remember that P starts with a maximum entropy *a priori* belief in E 's position at time t , where all points on E 's boundary curve are equally likely. We now consider for cases 1 through 4 what P 's *a posteriori* belief will be as to E 's position. The weighting functions (w_{old} and w_{new}) that we use can be varied to fit the application, as long as they sum to unity. In our examples, we set $w_{old}=0.2$ and $w_{new}=0.8$.

Case 1: Detection = TP & Conclusion = TP:

We have a detection in a position along the boundary arc where we expect to find E . As long as the distance between P and E is small enough that detection is more likely than a false alarm, we accept the detection as true. The new probability density function ($pdf_{1,new}$) associated with the reading has a probability 1 that E is within σ_r of the detection reading and probability 0 of being elsewhere. Our *a posteriori* belief function pdf_1 is a weighted average of $pdf_{1,new}$ with our *a priori* belief function pdf_{old} :

$$\begin{aligned}
pdf_1 &= w_{old}pdf_{old} + w_{new}pdf_{1,new} \\
pdf_{1,new} &= \begin{cases} 1 & \text{at that position} \\ 0 & \text{other positions} \end{cases} \quad (5.4a)
\end{aligned}$$

Case 2: Detection = TP & Conclusion = FP:

In this case we detect the target, but the distance from P to E is enough to make it more likely that the reading is a false alarm. We do not update our belief function so $pdf_2 = pdf_{old}$.

Case 3: Detection = FP & Conclusion = TP:

In this case, the false alarm returns a reading with coordinates such that the probability that the reading is TP is greater than the likelihood that it is FP. The reading must be within σ_r of E 's arc, and a distance d small enough that the Boolean statement $(Cd^\alpha > K_{FP}A_1/A_2)$ is true. We define a new *a posteriori* belief function pdf_3 such that:

$$\begin{aligned}
pdf_3 &= w_{old}pdf_{old} + w_{new}pdf_{3,new} \\
pdf_{3,new} &= \begin{cases} \text{uniform} & \text{all positions in } \sigma_r \text{ of } E\text{'s arc where } Cd^{-\alpha} > K_{FP}A_1 / A_2 \\ 0 & \text{other positions} \end{cases} \quad (5.4b)
\end{aligned}$$

Case 4: Detection = FP & Conclusion = FP:

The detection is a false positive and the conditions in Case 3 do not hold. Since we believe that the detection is false, we do not update the belief function. $pdf_4 = pdf_{old}$.

Case 5: Detection = ND & Conclusion = TN.

In this case, the radar does not detect the target and E 's arc based on our *a priori* information includes a region outside the effective sensing range. So, we think the evader is on E 's arc beyond the effective sensing range with a uniform distribution. We will update the belief function as follows:

$$pdf_5 = w_{old} pdf_{old} + w_{new} pdf_{5,new} \quad (5.4c)$$

$$pdf_{5,new} = \begin{cases} \text{uniform} & \text{at position outside } R_{sense} \\ 0 & \text{other positions} \end{cases}$$

Case 6: Detection = ND & Conclusion = FN.

In this case the radar does not detect the target, but our *a priori* knowledge says that E must be within the sensing range. Therefore, since we are certain that the reading is false, we do not update the belief function and $pdf_6 = pdf_{old}$.

Summary of six cases:

Base on these six cases, we use the probabilities and the probability distribution functions for each case to calculate the expected *a posteriori* belief function:

$$pdf_{Expected} = \sum_{i=1}^6 p_i pdf_i \quad (5.5)$$

As is typical for problems of this type, we initialize the system by setting the initial pdf_{old} to the maximum entropy solution, where all positions on the curves are equally likely.

5.2.3 Pursuit-evasion game solution

We use Shannon’s entropy function from information theory to calculate the amount of uncertainty [33] as to the location of E that a given pdf provides P . Using the expected probability distribution function from Equation (5.5):

$$Entropy = \sum_{\zeta = \text{all state in pdf}} - pdf(\zeta) \cdot \log(pdf(\zeta)) \quad (5.6)$$

where Equation (5.6) is summed over the set of points (or discrete regions) in E ’s arc. Higher entropy indicates more uncertainty. The evader E wants to maximize the entropy value (P ’s expected uncertainty) and the pursuer P wants to minimize it. E should therefore follow a game theoretic strategy [19] that maximizes the value of Equation (5.6).

We note here that when E ’s arc is wholly contained within P ’s effective sensing range the entropy of the *a posteriori* belief functions is low and almost uniform. This would lead to E making sub-optimal random choices. We note that in these situations, P ’s radar detects E from the strength of the radar signals E reflects. The shorter the distance, the stronger the energy is. In these cases, E (P) wants to minimize (maximize) the reflected radar signal energy, which is equivalent to maximizing (minimizing) the distance between P and E . We combine this with Equation (5.6) to provide the utility function with a balance variable λ that we use for our pursuit-evasion game:

$$payoff = Entropy - \lambda \cdot Energy \quad (5.7)$$

Inside the effective sensing range, the entropy value is near 0 and the energy value is large. Outside the effective sensing range, the energy value quickly falls to near zero, while the entropy metric increases. Equation (5.7) effectively expresses the conflict between P and E for both phases of the chase. We use $\lambda = 1$ for our simulation.

We now present the algorithm we use to find P and E 's optimal pursuit-evasion strategies for games relying on sensor data:

- Step 0: Calculate the maximum regions for pursuer and evader in time period T . Find the front boundary arcs for both regions. Divide P 's arc into $M-1$ equal sized segments by M discrete points. Divide E 's arc into $N-1$ equal sized segments by N discrete points. The initial probability distribution for P 's belief function is the maximum entropy pdf (i.e. $1/N$ for each N points), which is pdf_{old} for the first iteration.
- Step 1: For each pair (i, j) where $1 \leq i \leq M$ and $1 \leq j \leq N$, calculate the distance for the corresponding. Find probabilities p_i (Chapter 5.2.1) and *a posteriori* belief functions pdf_i (Chapter 5.2.2) for cases $i = 1 \dots 6$. Find the entropy (Equation (5.6)) for pair (i, j) . Then use the distance between the players to calculate the amount of P 's radar energy reflected by E . We denote the zero-sum game payoff matrix [19] as A . Set element (i, j) of A to $Entropy - \lambda * Energy$.
- Step 2: Use linear programming [19] to solve the two-person zero-sum game posed by A . The solutions of the linear programming problem are pdf 's for E and P . That denote the optimal mixed strategies that E (P) can use for maximizing (minimizing) the value of Equation (5.7). Use the probability distribution function of evader as pdf_{old} for the next iteration and repeat Step 1.
- Step 3: The algorithm stops when either E 's pdf in Step 2 converges or the number of iterations exceeds a threshold value.

At the end of this process, we have probability density functions that define the optimal mixed strategies for P and E . Each player can choose a random value between 0 and 1 then moves to the discrete point on the arc corresponding to this choice in the *pdf* [19]. By doing so, E can be certain that this process will maximize P 's uncertainty as to its position in the future. Similarly, P 's choice limits the amount of confusion E can cause.

For the example situation in Figure 5, E 's *pdf* will have a high probability of turning right to get away from the pursuer and a very low probability of turning left towards P . Similarly, P will be very likely to go straight and have low probabilities for turning either left or right.

In this approach, P and E decide their strategies for a sequence of finite time steps. The *pdf* at the end of each time step serves as the initial *pdf_{old}* for the next time step, instead of using a maximum entropy *pdf*. For the sake of expediency we divide the strategy choices and time steps into a set of discrete choices, instead of using continuous variables. Doing so allows us to directly apply a number of results from traditional game theory [19], which guarantee the existence of optimal strategies. It also allows us to use linear programming to compute the optimal strategies. This approach is based on the reasonable assumption that as the number of arc points (N and M) and the number of time segments grow, the results will converge towards the solution of the corresponding continuous problem.

5.3 Strategy for Games with Perfect Information

To verify the utility of this approach, we contrast it with equivalent strategies for games with perfect information. For these games, P and E choose strategies based solely on the distance between the two players. Since the reflected signal strength is a function of the distance. Minimizing (maximizing) the distance is the same as minimizing (maximizing) reflected signal strength.

First, each player detects the other player's position either from radar readings or by using *a priori* knowledge. This *a priori* knowledge includes the results of previous radar readings. Each player then calculates the arcs for both players. These arcs are used to populate a zero-sum payoff matrix, similar to the one constructed in Step 1 of Chapter 5.2.3. The value (i, j) in this payoff matrix is simply the distances between the discrete points of E 's arc point i and P 's arc point j . Minimax (Maximin) of the distance between P 's (E 's) positions is used to find optimal mixed solutions for P (E). E tries to move to point furthest away from P , to avoid capture as long as possible. P tries to minimize its distance from E and capture it.

5.4 Experimental Results

To evaluate this approach, we created simulations of this game in MATLAB. Simulations were run for all for possible combinations of strategies:

- ◆ Information theory utility function vs. information theory utility function;
- ◆ Information theory utility function vs. perfect information utility function;
- ◆ Perfect information utility function vs. information theory utility function;

- ◆ And perfect information utility function vs. perfect information utility function.

In the following figures, Red is the evader E , which starts at position $(0, 70)$ heading $y+$ axis or $(-10, 60)$ heading $x+$ axis. Blue is the pursuer P , whose initial position is $(0, 0)$. Red circles (blue squares) show E 's (P 's) actual positions. Red crosses (blue pluses) are E 's (P 's) position as perceived by their opponent. If the cross and square (plus and circle) overlap, then E (P) correctly perceived the opponent's position. Otherwise, their interpretation was wrong. We compare the entropy strategy with the perfect information strategy for both players. Figures 5.2 through 5.5 show the results from sample simulation runs.

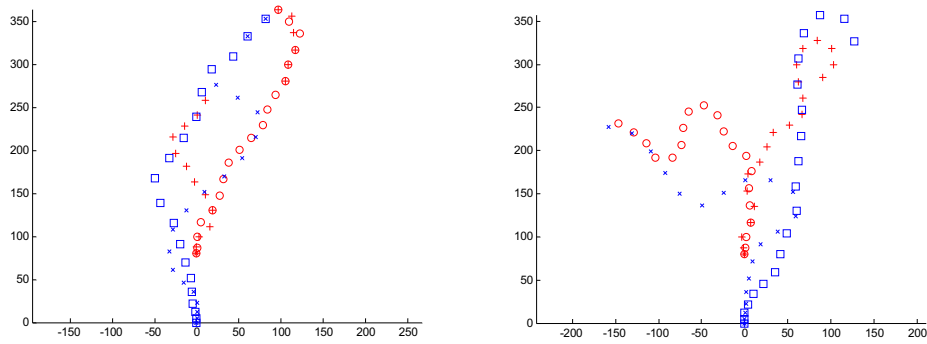


Figure 5.2: P entropy strategy vs. E entropy strategy. Left: P found E ; Right: P lost E .

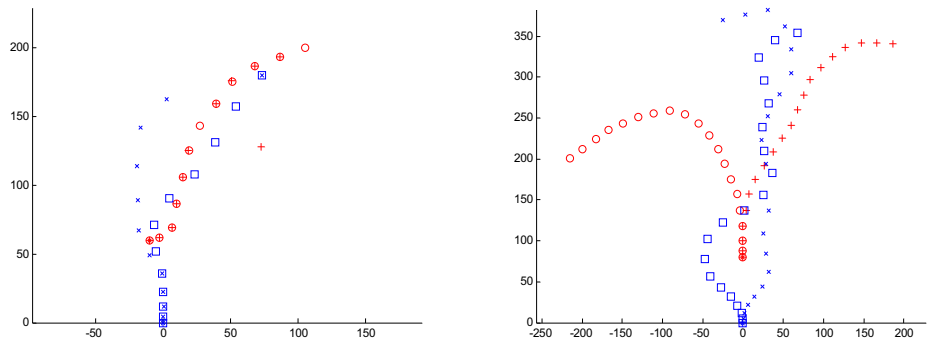


Figure 5.3: P entropy strategy vs. E perfect sensor strategy. Left: P found E ; Right: P lost E .

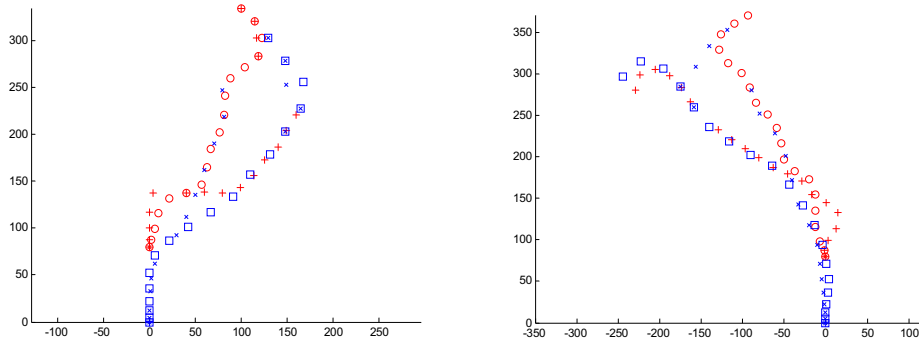


Figure 5.4: P perfect sensor strategy vs. E entropy strategy. Left: P found E ; Right: P lost E .

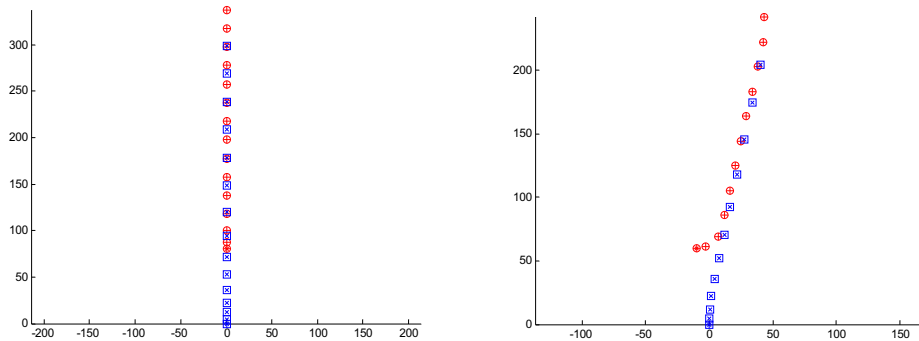


Figure 5.5: P and E both perfect sensor strategy. P found E .

We ran 36 repetitions of each scenario to calculate the mean chance for P to capture E . Table 5.2 contains the variance, standard deviation and the 95% confident intervals for the mean. Table 5.3 presents the mean values for each combination of strategies. These results indicate that if P uses the entropy based utility function, E is better to use perfect information strategy. But, if P uses the perfect information strategies it is guaranteed to perform better than when using the entropy based approach. Similarly

when P uses the perfect information approach, there is a very large incentive for E to use the entropy based utility function. These results indicate two things:

- ◆ Considering the sensor errors is very important for the evader.
- ◆ The pursuer's interests are not adequately represented in the information theory based payoff matrix.

We could, however, consider the game not as a zero-sum game with one payoff matrix. It appears that the game is better summarized as a bi-matrix game where the pursuer's strategy is based on the perfect information payoff matrix and the evader's strategy uses the payoff matrix from the information theoretic approach. Table 5.3 shows the likelihood of P 's capturing E for all four possible combinations of the two game strategies (perfect information and entropy based) and two different sets of initial conditions. These results are illustrative of all the tests we have run.

E intl.	(0,70) heading $Y+$				(-10,60) heading $X+$			
P vs. E	per - ent	per - per	ent - ent	ent - per	per - ent	per - per	ent - ent	ent - per
mean	0.5833	1.0000	0.4167	0.3056	0.8056	1.0000	0.5833	0.3333
found	21	36	15	11	29	36	21	12
Var.	0.2500	0.0000	0.2500	0.2183	0.1611	0.0000	0.2500	0.2286
Std.	0.5000	0.0000	0.5000	0.4672	0.4014	0.0000	0.5000	0.4781
CI. L	0.4200	1.0000	0.2533	0.1529	0.6744	1.0000	0.4200	0.1772
CI. U	0.7467	1.0000	0.5800	0.4582	0.9367	1.0000	0.7467	0.4895

Table 5.2: Mean, variance, standard deviation, upper and lower 95% confidence interval bounds for P 's ability to capture E in the four different scenarios.

	<i>P</i> ent.	<i>P</i> per.		<i>P</i> ent.	<i>P</i> per.
<i>E</i> ent.	0.4167	0.5833	<i>E</i> ent.	0.5833	0.8056
<i>E</i> per.	0.3056	1.0000	<i>E</i> per.	0.3333	1.0000

Table 5.3: Capture rate from each combination of strategies with different initial conditions.

The results in Table 5.3 indicate that the problem should best be modeled as a bi-matrix game [19]. It is always advantageous for the pursuer to use the strategy that assumes perfect information, and it is always advantageous for the evader to use the entropy based strategies in order to exploit the pursuer's sensing limitations.

CHAPTER SIX

PURSUIT-EVASION WITH ELECTRONIC COUNTER MEASURES

6.1 Effect of Electronic Counter Measures

As mentioned in Chapter 1, there exists a number of Electronic Counter Measures (ECM) where one participant can intentionally disrupt the sensing capability of their opponent. Two main ECM methods are to decrease the true positive rate or increase the false positive rate. The approach presented earlier in this chapter can be modified to find optimal ECM deployment strategies.

The use of chaff and aerosols is easy to integrate into our approach by adding rows to payoff matrix A (see Step3 of the algorithm in Chapter 5.2.3) corresponding to modifications of the p_i and pdf_i for the 6 cases (TP TP, TP FP, FP TP, FP FP, TN, FN) caused by increased false positive rates for chaff, or decreased true positive rates for aerosols. The false positive rate could be increased to a high percentage. 0% false positive rate means the radar will not have any Type II errors, while 100% means the radar has Type II errors continuously. The true positive rate could be reduced by a certain percentage; a 0% true positive rate reduction means the ECM has no effect and 100% reduction produces the radar never detects the target.

During the game, the pursuer will not know whether the evader is using the ECM or not. Thus, the pursuer will use the nominal true positive and false positive rates to calculate its payoff matrix. Since the evader knows when the ECM is active, it calculates the payoff matrix in a way that reflects whether the ECM is active or not.

When the players' radars read the positions of their opponent, any active ECM affects the readings. Since the TP and FP rates are based on the distance between the two players, the evader initiates its ECM as a function of its distances from the pursuer.

6.2 Experimental Results

To evaluate this approach, we created simulations of this game in MATLAB. In [3], we found that the pursuer is better served by following a strategy that minimizes the distance between itself and the perceived future position of the evader, while the evader is better served by following a strategy based on maximizing the uncertainty of pursuer's knowledge of the evader's future position. So in these simulations with ECM, we use a distance-based strategy for the pursuer and an entropy-based strategy for the evader.

In the example presented here, the evader E starts at position $(0, 70)$ heading in the positive direction along the y axis and the pursuer P is initially at position $(0, 0)$ heading in the positive direction along the y axis. The evader initiates the ECM when its distance from the pursuer reaches a threshold value. The pursuer's maximum velocity is 30 meters per second and maximum acceleration is 3 meters per second squared. The evader's maximum velocity is 20 meters per second and maximum acceleration is 5 meters per second squared. We vary this value from 60 to 150 meters with intervals of 5 meters for each combination of TP and FP. The whole game lasts for 20 seconds and the ECM is active for up to 5 seconds. If the pursuer and evader are within 47 meters, we say that pursuer captures the evader. Note that the word "capture" is different from what it

means in Chapter 4 and [2]. It means that the sensing factor is too low to affect the pursuer-evasion game and the game will move to the scenario with perfect information.

We did three simulations. In the first simulation, we multiplied the true positive rate by a percentage of 0 and values varying from 10% to 100% with intervals of 15%. The nominal false positive rate is 0.02 (see Figure 6.1). For each combination of the modified TP, nominal FP and ECM starting distance, we ran 100 repetitions to calculate the mean chance for P to capture E and the 95% confident intervals for the mean. In the second simulation, we used false positive rates of zero and varying from 15% to 90% with intervals of 15% and used the nominal true positive rate. For each combination of the nominal TP, modified FP and ECM starting distance, we ran 100 repetitions to calculate the mean chance for P to capture E and the 95% confident intervals for the mean (see Figure 6.2). In the third simulation, we integrated the first and the second simulations. We multiplied the true positive rate by a percentage varying from 0% to 70% in intervals of 10% and varied the false positive rate from 10% to 90% with intervals of 10%. For each combination of the modified TP, modified FP and ECM starting distance, we ran 100 repetitions to calculate the mean chance for P to capture E and the 95% confident intervals for the mean (see Figure 6.3).

The following figures show some of these combinations. In the figures, the x -axis represents the ECM starting distance and y -axis represents the average capture percentage. The error bars show the 95% confident intervals. The TP and FP for the ECM time steps are written at the top. K_{ecm} is the false positive rate and C_{ecm} is the coefficient of true positive rate during the ECM is active.

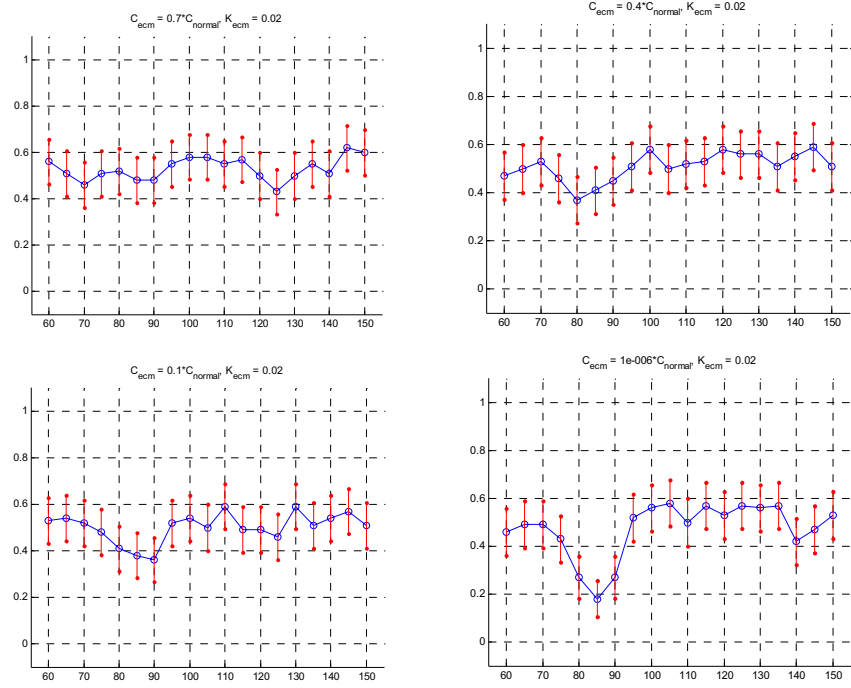


Figure 6.1: Results for the first simulation using the nominal false positive rate.

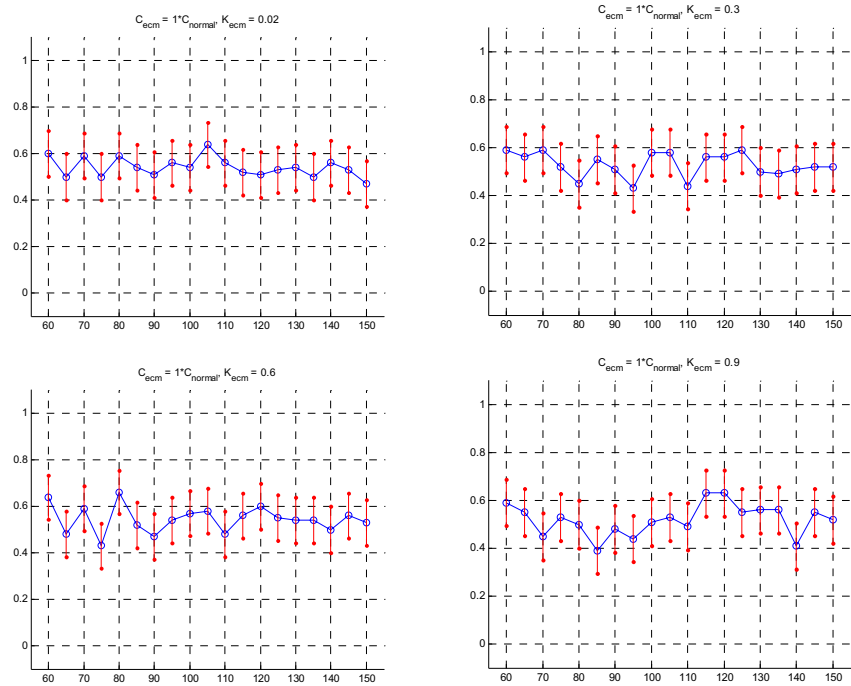


Figure 6.2: Results for the second simulation using nominal true positive rate.

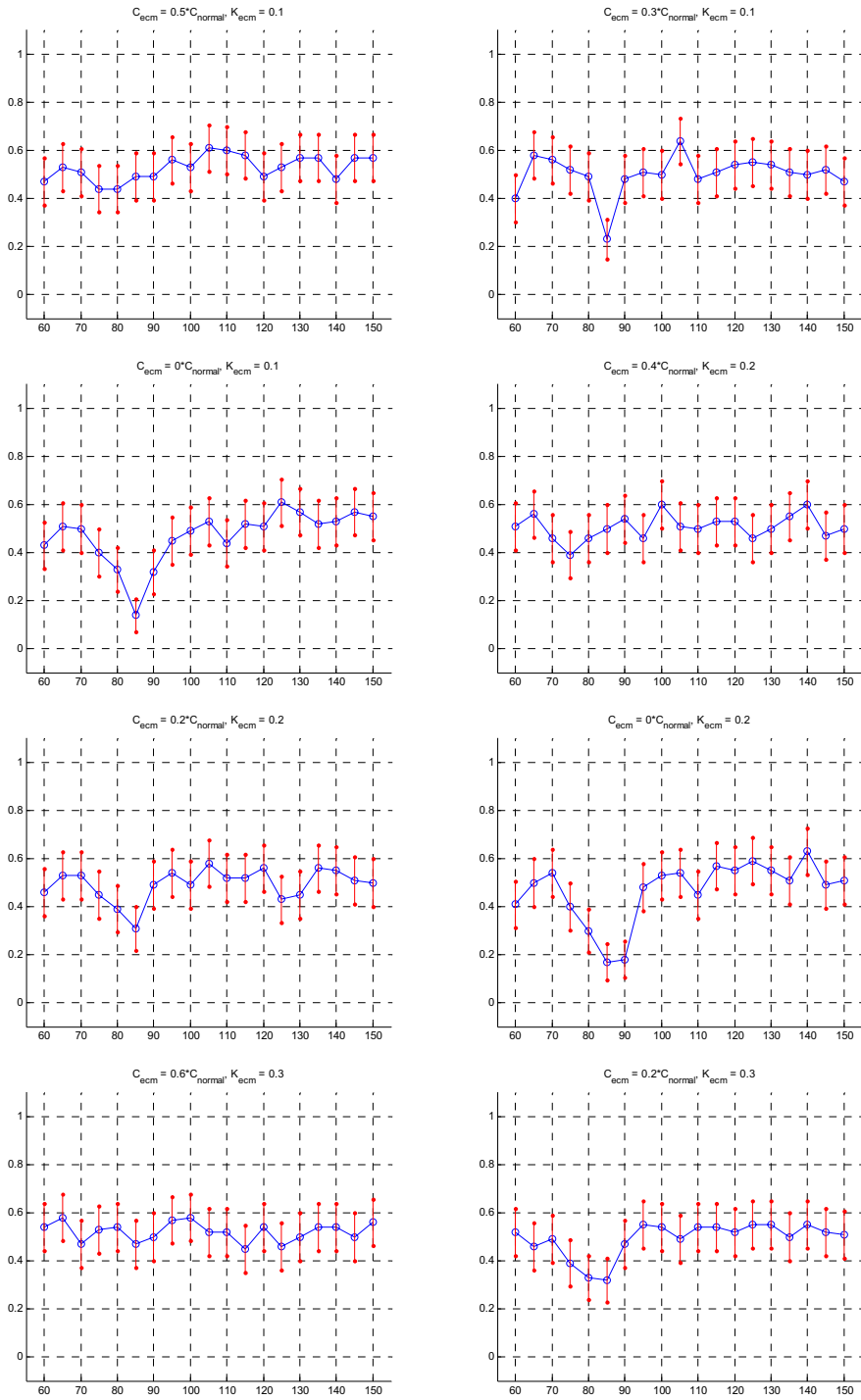


Figure 6.3: Simulation results for representative combinations of TP and FP rates.

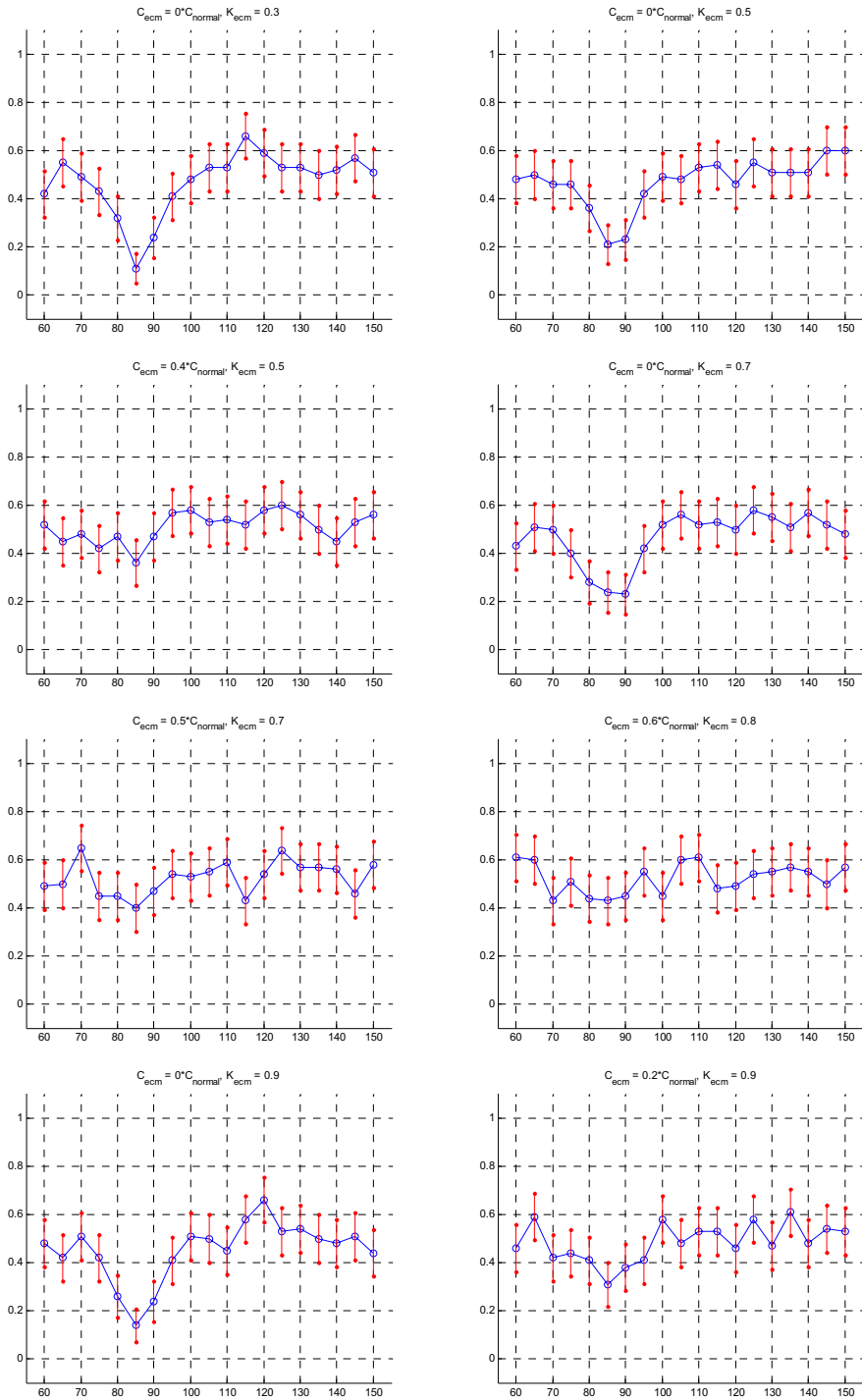


Figure 6.3: Simulation results for representative combinations of TP and FP rates
(Continued).

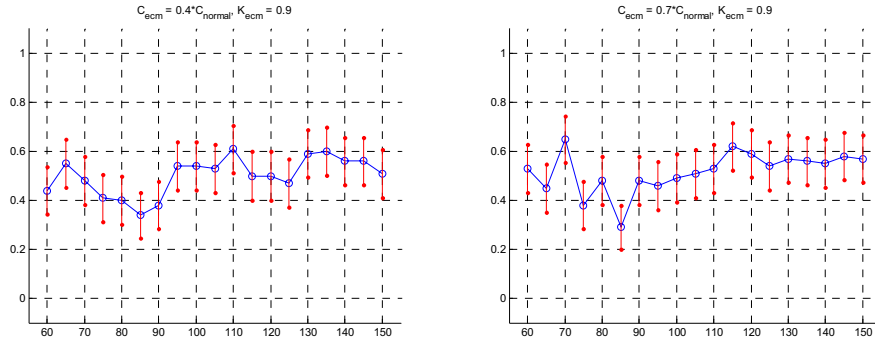


Figure 6.3: Simulation results for representative combinations of TP and FP rates (Continued).

From the simulation, we want to find the distance where the evader should start the ECM. If we can find a distance where the capture percentage is significantly lower than the other cases, the evader's best option is to initiate the ECM at that distance.

Figure 6.1 shows the results of using varying the true positive rate using ECM. The effect of the ECM becomes significant as the true positive rate decreases. Figure 6.2 shows the results of varying the false positive rate. We note that these ECM do not significantly change the evader's success rate. Figure 6.3 shows results combining these two ECM approaches. We find that the ECM influence is more significant when we decrease the true positive rate for a given false positive rate, but it is less significant if we increase the false positive rate for a given true positive rate.

Decreasing the true positive rate appears to be more effective than increasing the false positive rate. There are two main reasons for this:

- ◆ The probability that a false positive is accepted as a true positive is the area along the evader's front boundary divided by the area of pursuer's sensing range [3]. This is small, so that very few false positives are incorrectly classified.

- ◆ If the false positive is accepted as a true positive, the incorrect sensed position of evader is closed to evader's actual position. Thus, even if the evader increases the false positive rate, it does not greatly degrade the pursuer's actionable information.

We note that these two reasons are a consequence of our game definition. Since this is a pursuit evasion game, we assume that both parties know the positions of their opponents at the start of the game. In other applications, we expect the false positive ECM to be more effective.

We also note that the capture rate is particularly low when the ECM is triggered at a distance of around 85 to 90 meters. In our simulation, the nominal sensing range is 125 meters, and maximum velocity of pursuer and evader are 30 and 20 meters per second, respectively. Consider the situation when the distance between them is 85 meters and pursuer is heading towards evader. As shown in Figure 6.4, with the pursuer at point P_1 and the evader at point E_1 . When the evader turns on the ECM for 5 time steps and the pursuer assumes the evader continues along a straight line, then the pursuer travels to point P_2 . But if the evader turns, it will reach point E_2 . The distance between P_2 and E_2 is approximately 125, which is the pursuer's nominal sensing range. If the pursuer turns but the evader goes straight, the distance between their future positions is also approximately the nominal sensing range. So, when the evader initiates the ECM at a range where it can exit the pursuer's sensing range while the ECM is active, that strategy significantly lowers the pursuer's capture rate.

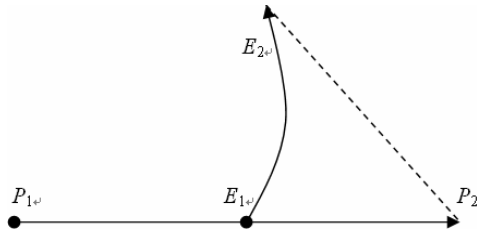


Figure 6.4: Geometry explains why starting distance 85 has significant low capture rate.

To verify the utility of this approach, we construct a fourth simulation, where both pursuer and evader use perfect-information-based strategies. In this game, the pursuer and evader strategies are both based solely on the distance between them. The opponents' position is determined by combining the radar readings and the *a priori* information. We multiplied the true positive rate by a percentage varying from 0% to 100% with intervals of 10% and varied the false positive rate being 0.02 and from 10% to 90% with intervals of 10%. The configurations are similar to the 3rd simulation. Figure 6.5 shows some simulation results.

From Figure 6.5, the simulation shows that decreasing the TP rate is more effective than increasing the FP rate. The decision does not rely on the entropy or uncertainty. The ECM is not affecting their strategies. But it does affect the sensor reading. And we can see the pursuer has a zero capture rate if the evader starts ECM at distance 90 meters and the TP is zero. Also, when we compare this to the result in [2, 9], we see the ECM can reduce the capture rate when the pursuer no longer has information about the evader even if the pursuer satisfies the capture criteria in [2, 6].

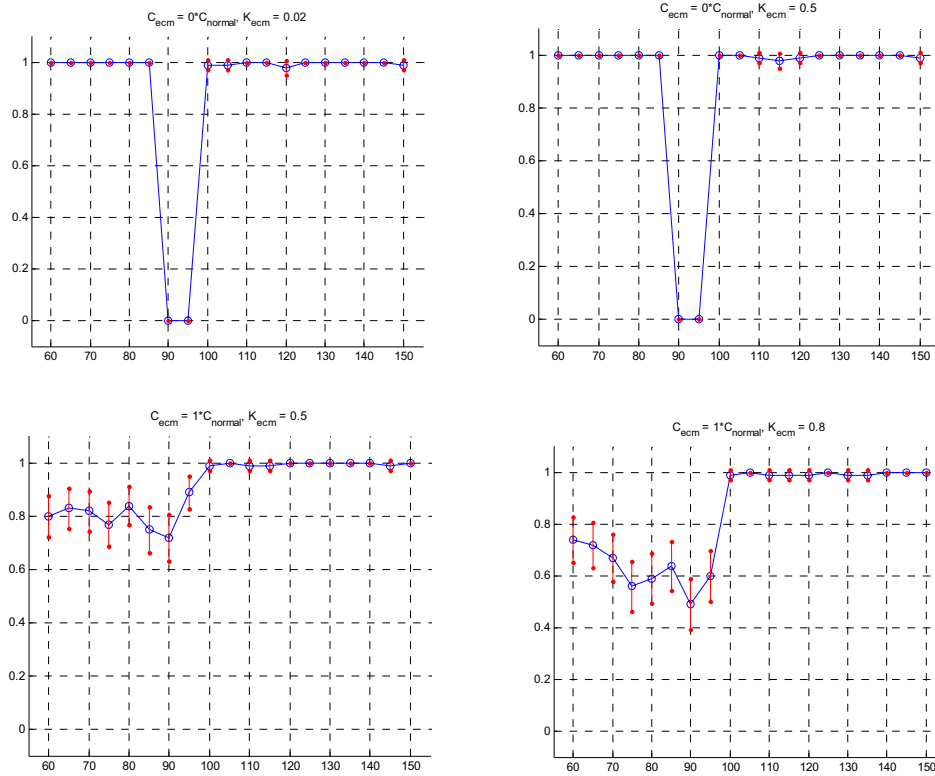


Figure 6.5: Simulation results for ECM where P and E use perfect-information strategies.

CHAPTER SEVEN

CONCLUSION AND FUTURE RESEARCH

In this thesis, I extended the classical pursuit-evasion problem by adding acceleration and turning constraints, this makes the problem more closely match the physics of the problem. I then found the criteria for both capture and escape, thus solving the game of kind. I then included sensing limitations, which introduces a new layer of complexity into the analysis. The optimal strategies I found for both the pursuer and evader have a number of practical applications. Finally, Electronic Counter Measures (ECM) were added to the problem, reflecting modern combat realities. Optimal strategies for evader use of ECM are derived and presented. Interestingly, the ECM game, although clearly adversarial, is not strictly zero-sum.

The work in this thesis considers one-on-one pursuit-evasion games in an unoccluded 2-D plane. We updated previous studies of pursuit-evasion games by removing the constraints that both players have a fixed velocity. This makes the problem more realistic for many applications. It also provides new insights into the conditions for capture previously reported in [6]. Based on these insights, we found the criteria that determine the games of kind for this problem (i.e. the conditions necessary for a given player to win) for the capture under new conditions and constraints theoretically. Figure 7.1 uses a flow chart to summarize our results. As we have noted, since the largest class of practical 3-D problems reduces to the 2-D case our work is also relevant in that domain.

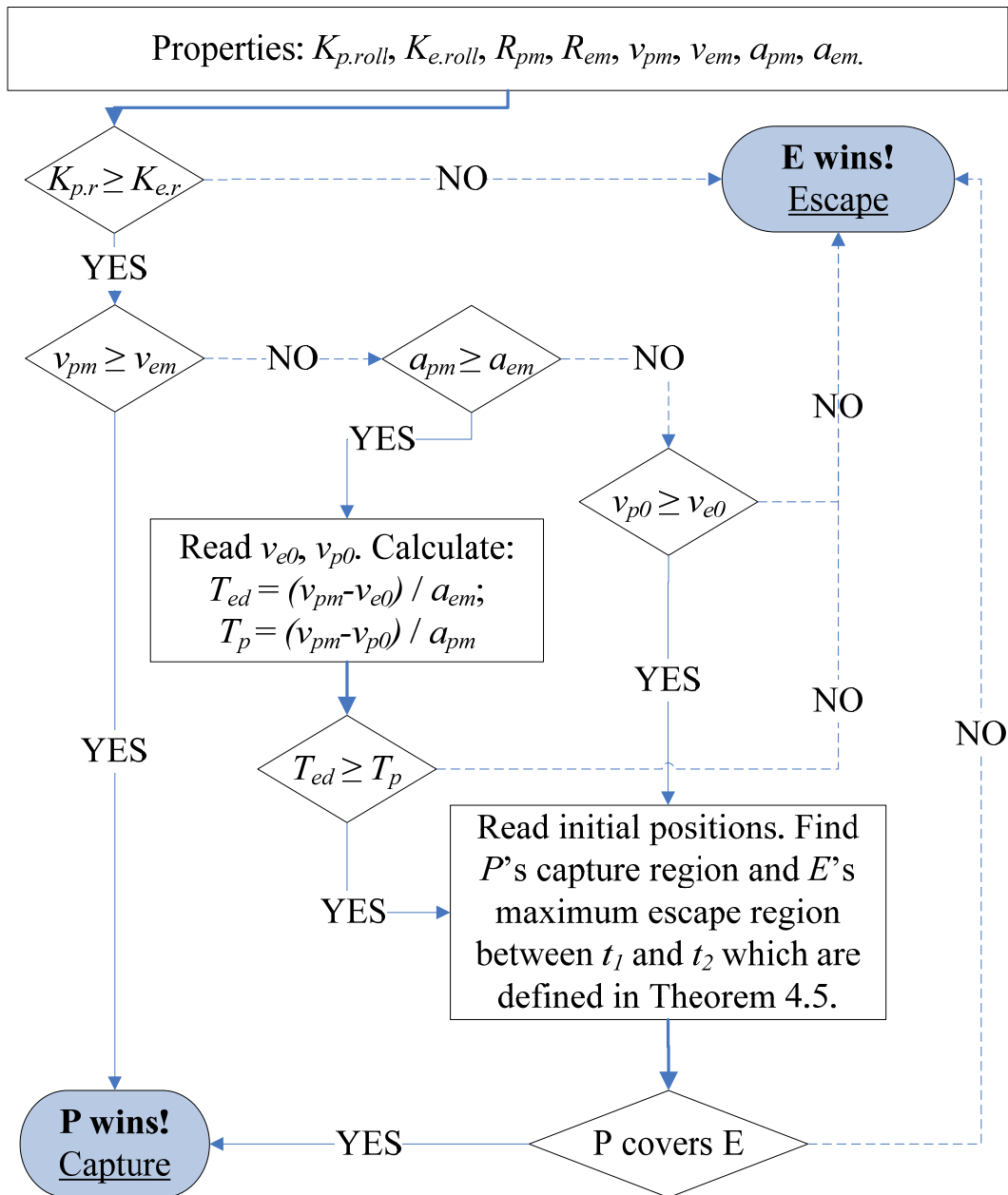


Figure 7.1: A flow chart that summarizes the games of kind for pursuit-evasion games with acceleration.

In the pursuit and evasion game with perfect information in Chapter 4, it is easy to see that if the pursuer has a larger maximum velocity than the evader, the pursuer will

eventually overtake the evader as time progresses. The evader will therefore go to the position furthest from the evader to prolong the time until capture. But in the game without perfect information in Chapter 5, the evader is not constrained to follow that strategy. It is better served by following a mixed strategy that is more unpredictable. By maximizing the pursuer's uncertainty about its current position, it can eventually reach a state where the pursuer has no knowledge of its position, effectively escaping from the fastest pursuer. Our simulation results illustrate the utility of this approach.

It is interesting to note that the same utility function does not define an optimal strategy for the pursuer. The pursuer is better served by following a strategy that minimizes the distance between itself and the perceived future position of the evader. It makes sense that this approach places the pursuer at a point well suited to eventually overtake the evader. This position will also, as a by-product, tend to have a higher true positive detection rate, which is also advantageous for the pursuer. Both of these conclusions are supported by our simulation results. This implies that the pursuit evasion game without perfect knowledge is not a truly zero-sum game, since the perfect information strategies are more advantageous for the pursuer than the zero sum game defined by the entropy-based utility function.

It is amusing to note that using information theory notation; the pursuer (evader) should try to minimize (maximize) the information contained in its sensor readings. This is quite true (although it seems to be an oxymoron), since the pursuer (evader) attempts to make the evader's future positions predictable (random).

In Chapter 6, we allow the evader to use electronic counter measures (ECM) that modify the true positive and false positive error rates of the pursuer's radar.

We assume that both players know their opponent's initial positions because this is a pursuit-evasion game instead of a search game. Our simulations indicate that in this game the evader is better served by using ECM technologies that decrease the true positive rate rather than increasing the false positive rate. Also, the pursuer is better served by following a strategy that minimizes the distance between itself and the perceived future position of the evader. First, this approach places the pursuer at a point well suited to eventually overtake the evader. Second, this position will also, as a by-product, tend to have a higher true positive detection rate, which is also advantageous for the pursuer. Third, since the evader can modify the parameters of the pursuer's radar, the information theory entropy metric the pursuer can compute concerning the evader's future positions may be based on incorrect assumptions. The pursuit evasion game with ECM is not a truly zero-sum game, since the perfect information strategies are more advantageous for the pursuer than the zero sum game defined by the entropy-based utility function. This is a consequence of the information imbalance inherent in the game; i.e., the evader always has more information than the pursuer.

The approach presented here solves this continuous problem by using a discrete approximation. Although this is expedient, and more easily understood, it would be useful to solve the continuous problem directly. On the other hand, it is also straightforward to analyze the continuous problem numerically by creating ever-finer approximations.

Another worthwhile extension would be to relax our assumption that vehicles always move at the fastest reachable velocity. It should be possible to do this by not looking solely at the boundary arc for each player, but rather integrating over the entire area each player could reach from their initial starting point. We suspect that this could be done more easily in the continuous domain. We suspect, as well, that the results obtained would not greatly differ from those presented here.

In this thesis, we assume the noise is uncorrelated, which is not always true, but can simplify the problem. It would be worthwhile to use the theoretical approach to modeling signal propagation in complex environments presented in [34, 35] to extend this approach. The resulting strategies should be well suited to pursuit evasion problems in urban settings, where signals are subject to fading. That extension should also be relatively straightforward. Similarly, we plan on extending this work to include occlusion based sensing problems like those in [15, 16].

The Ph.D. dissertation [17] analyzing the use of decoys in pursuit evasion games is the only relevant research currently available in this domain. Electronic Counter Measure pursuit-evasion is an important application domain and the questions as to what types of ECM are most useful for this class of games is interesting, since this is a very practical way of analyzing deception problems in the larger theory of games.

Finally, we plan on extending this approach in the near future to the analysis of the three-dimension pursuit-evasion game. Vehicles that move in 3-dimensions have six degrees of freedom: In addition to movement in the x, y, and z directions, pitch, roll, and yaw are degrees of freedom. Most conventional aircraft and high-speed missiles have

limited yaw rates and therefore perform bank-to-turn maneuvers to avoid using the yaw degree of freedom. The results in [24] use this insight to show how the 3-D pursuit-evasion problem reduces to the 2-D problem for these classes of aircraft. They show how to calculate critical values for the differences between the roll rates of the pursuer and evader. If the pursuer's roll rate is not sufficiently larger than the evader's, the evader will escape. But if the pursuer's roll rate is sufficiently greater than the evader's, the pursuer has optimal maneuvers that allow it to constrain the evader to maneuvers within the same xy plane. It is straightforward, therefore, to adapt the two dimensional analysis given here for use by most aircraft.

APPENDICES

Appendix A

Circle Involute Background

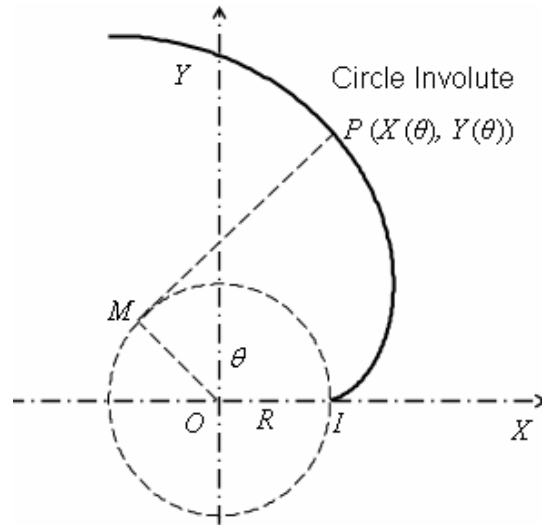


Figure A-1: The circle involute (bold curve) is formed by taking a line segment of a fixed length and wrapping it around a circle of a fixed radius. Angle $\theta = \angle IOM$, Line $IO = R$.

The equation for a circle involute (see Figure A-1) with respect to the tangent angle θ is:

$$\begin{aligned} X(\theta) &= R \cdot (\cos \theta + \theta \cdot \sin \theta) \\ Y(\theta) &= R \cdot (\sin \theta - \theta \cdot \cos \theta) \end{aligned} \quad (\text{A1})$$

The length of the arc IP it traces is:

$$s(\theta) = \frac{1}{2} R \cdot \theta^2 \quad (\text{A2})$$

Appendix B

Analysis of Non-Critical Path Optimal Paths

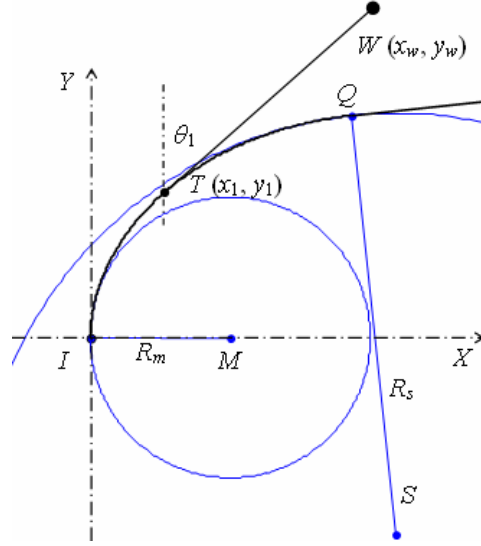


Figure B-1: Use different acceleration to reach tangent point T and go straight to point W .

The equations of Critical Path with respect to time t are:

$$\begin{aligned}
 \varphi(t) &= \frac{K}{a_m} (\log(v_0 + a_m t) - \log(v_0)) \\
 x(t) &= \frac{(v_0 + a_m t)^2}{4a_m^2 + K^2} [2a_m \sin(\varphi(t)) - K \cos(\varphi(t))] + \frac{Kv_0^2}{4a_m^2 + K^2} \\
 y(t) &= \frac{(v_0 + a_m t)^2}{4a_m^2 + K^2} [2a_m \cos(\varphi(t)) + K \sin(\varphi(t))] - \frac{2a_m v_0^2}{4a_m^2 + K^2} \\
 &\text{given } 0 \leq t \leq (v_m - v_0)/a_m, \quad v_s \leq v_0 \leq v_m.
 \end{aligned} \tag{B1}$$

Find the time from point I to W by varying the acceleration from zero to a_m . Use the acceleration with Equation (B1), to find the equivalent of the critical path. Let $(x(t), y(t))$ be a position on the path and $\theta(t)$ be the direction of the vehicle on that position.

Draw a tangent line from W to the curve with intersection at point T . Suppose the time from initial position to T is t_1 and from T to W is t_2 . We can derive the minimal time path by using the following equations:

$$\begin{aligned}
\tan(\theta_1) &= (x_1 - x_w)/(y_1 - y_w) \\
\theta_1 &= \frac{K}{a}(\log(v_0 + at_1) - \log(v_0)) \\
x_1 &= \frac{(v_0 + at_1)^2}{4a^2 + K^2} (2a \sin \theta_1 - K \cos \theta_1) + \frac{Kv_0^2}{4a^2 + K^2} . \\
y_1 &= \frac{(v_0 + at_1)^2}{4a^2 + K^2} (2a \cos \theta_1 + K \sin \theta_1) - \frac{2av_0^2}{4a^2 + K^2} \\
0 \leq t_1 &\leq (v_m - v_0)/a, \quad v_s \leq v_0 \leq v_m \\
\text{Let } v_1 &= v_0 + at_1 \\
di &= \sqrt{(x_w - x_1)^2 + (y_w - y_1)^2} \\
da &= (v_m^2 - v_1^2)/(2a_m) \\
\text{if } da > di, &\text{ solve } v_1 t_2 + a_m t_2^2 / 2 = di \text{ for } t_2 \\
\text{if } da \leq di, &t_2 = (v_m - v_1)/a_m + (d_i - d_a)/v_m
\end{aligned} \tag{B2}$$

Then $t_1 + t_2$ is the time from point I to point W . Now minimizing $t_1 + t_2$ involves solving a nonlinear program in Equation (B2). Techniques like Newton's method can find the optimal solution.

REFERENCES

- [1] M. H. Breitner, "The Genesis of Differential Games in Light of Isaacs Contributions," *Journal of Optimization Theory and Applications*, vol. 123, no. 4, pp. 523-559, Mar, 2005.
- [2] R. R. Brooks, Jing-En Pang, and C. Griffin, "Pursuit and evasion Game with acceleration," submitted for review, Oct, 2006.
- [3] R. R. Brooks, Jing-En Pang, and C. Griffin, "Pursuit and Evasion without Perfect Knowledge", submitted for review, Oct, 2006.
- [4] R. R. Brooks, Jing-En Pang, and C. Griffin, "Game Theory and Information Theory Analysis of Electronic Counter Measures in Pursuit-Evasion Games", submitted for review, Mar, 2007.
- [5] R. R. Brooks, Autonomous Weapons Platform Controller, Clemson University Technical Report, Jan, 2006.
- [6] E. Cockayne, "Plane Pursuit with Curvature Constraints", *SIAM Journal on Applied Mathematics*, vol. 15, no. 6, pp. 1511-1516, Nov, 1967.
- [7] K. Fregene, D. C. Kennedy, and D. W. L. Wang, "Toward a Systems- and Control-Oriented Agent Framework," *IEEE Transactions on Systems, Man, and Cybernetics, Part B*, vol. 35, no. 5, pp. 999-1012, Oct, 2005.
- [8] W. M. Getz and M. Pachter, "Capturability in a Two-Target Game of Two Cars", *Journal of Guidance and Control*, vol. 4, no. 1, pp. 15-21, Jan-Feb, 1981.
- [9] R. Isaacs, *Differential Games*, Dover Publications, Mineola, NY, 1965.
- [10] V. Isler, S. Kannan, and S. Khanna, "Randomized Pursuit-Evasion in a Polygonal Environment", *IEEE Transactions on Robotics and Automation*, vol. 21, no. 5, pp. 875-884, Oct, 2005.
- [11] V. Isler, S. Kannan, and S. Khanna, "Randomized Pursuit-Evasion with Local Visibility", *SIAM Journal on Discrete Mathematics*, vol. 20, no. 1, pp. 26-41, 2006.
- [12] P. Kachroo, S. A. Shedied, J. S. Bay, and H. Vanlandingham, "Dynamic Programming Solution for a Class of Pursuit Evasion Problems: The Herding Problem", *IEEE Transactions on Systems, Man, and Cybernetics, Part C: Applications and Reviews*, vol. 31, no. 1, pp. 35-41, Feb, 2001.

- [13] P. Kachroo, S. A. Shediad, and H. Vanlandingham, "Pursuit Evasion: The herding Noncooperative Dynamic Game—The Stochastic Model", *IEEE Transactions on Systems, Man, and Cybernetics, Part C: Applications and Reviews*, vol. 32, no. 1, pp. 37-42, Feb, 2002.
- [14] J. Karelahti, K. Virtanen, and T. Raivio, "Game Optimal Support Time of a Medium Range Air-to-Air Missile", *Proc. of the 11th International Symposium on Differential Games and Applications, International Society of Dynamic Games*, Tucson, Arizona, 2005.
- [15] S. M. LaValle, D. Lin, L. J. Guibas, J. C. Latombe, and R. Motwani, "Finding an unpredictable target in a workspace with obstacles", *Proceedings of the 1997 IEEE International Conference on Robotics and Automation*, pp. 737-742, 1997.
- [16] S. M. LaValle and J. E. Hinrichsen, "Visibility-Based Pursuit-Evasion: The Case of Curved Environments", *IEEE Transactions on Robotics and Automation*, vol. 17, no. 2, pp. 196-202, Apr, 2001.
- [17] J. Lewin, *Decoy in Pursuit Evasion Games*, Ph. D. Dissertation, Department of Aeronautics and Astronautics, Stanford University, 1973.
- [18] J. Lewin and G. J. Olsder, "Conic Surveillance Evasion", *Journal of Optimization Theory and Applications*, vol. 27, no. 1, pp. 107-125, 1979.
- [19] E. Mendelson, *Introducing Game Theory and Its Applications*, Chapman & Hall / CRC, Boca Raton, FLA, 2004.
- [20] A. W. Merz, *The Homicidal Chauffeur - A Differential Game*, Ph.D. Dissertation, Stanford University, Dept. of Aeronautics and Astronautics, 1971.
- [21] A. W. Merz, "The game of two identical cars", *Journal of Optimization Theory and Applications*, vol. 9, no. 5, pp. 324-343, 1972.
- [22] A. W. Merz and D. S. Hague, "Coplanar Tail-Chase Aerial Combat as a Differential Game," *AIAA Journal*, vol. 15, no. 10, pp. 1419-1423, Oct, 1977.
- [23] A. W. Merz, "To Pursue or to Evade—That is the Question", *Journal of Guidance, Control, and Dynamics*, vol. 8, no. 2, pp. 161-166, Mar-Apr, 1985.
- [24] T. Miloh, M. Pachter, and A. Segal, "The Effect of a Finite Roll Rate on the Miss-Distance of a Bank-to-Turn Missile", *Computers and Mathematics with Applications*, vol. 26, no. 6, pp. 43-54, 1993.

- [25] T. Muppirlala, R. Murrieta-Cid, and S. Hjtchinson, “Optimal Motion Strategies Based on Critical Events to Maintain Visibility of a Moving Target”, *IEEE International Conference on Robotics and Automation (ICRA)*, 2005.
- [26] V. S. Patsko and V. L. Turova, “History of the Homicidal Chauffeur Problem”, <http://home.imm.uran.ru/kumkov/HHCP/index.html>, last visited on Feb, 2007.
- [27] T. Raivio and J. Ranta, “Optimal Missile Avoidance Trajectory Synthesis in the Endgame,” *AIAA 2002-4947 AIAA Guidance, Navigation and Control Conference*, Monterey, CA, Aug, 2002.
- [28] P. Setlur, J. Wagner, D. Dawson and D. Braganza, “A Trajectory Tracking Steer-by-Wire Control System for Ground Vehicles”, *IEEE Transactions on Vehicular Technology*, vol. 55, no. 1, pp. 76-85, Jan. 2006.
- [29] L. D. Stone, *Theory of Optimal Search*, Mathematics in Science and Engineering, vol. 118, Academic Press, NY, 1975.
- [30] D. Swanson, “Environmental Effects,” Chapter 11, *Distributed Sensor Networks*, eds. S. S. Iyengar, R. R. Brooks, CRC Press, Boca Raton, FLA, 2005.
- [31] R. Vidal, O. Shakernia, H. Jin Kim, David H. Shim, and Shankar Sastry, “Probabilistic Pursuit-Evasion Games: Theory, Implementation, and Experimental Evaluation”, *IEEE Transaction on Robotics and Automation*, vol. 18, no. 5, pp. 662- 669, Oct, 2002.
- [32] A. R. Washburn, *Search and Detection*, 4th ed., Military Application Society of the Institute of Operations Research and Management Science, Linthicum, MD, 2002.
- [33] E. W. Weisstein, *CRC Concise Encyclopedia of Mathematics*, CRC Press, Boca Raton, FLA, 1999.
- [34] K. Yao, “A Representation Theorem and Its Applications to Spherically Invariant Random Processes,” *IEEE Transactions on Information Theory*, vol. IT-19, no. 5, pp. 600-608, Sep, 1973.
- [35] K. Yao, M. Simon, and E. Biglieri, “A Unified Theory on the Modeling of Wireless Communications Fading Channel Statistics,” *Proceedings CISS*, Princeton, NJ, Mar, 2004.
- [36] F. Zhao and L. Guibas, *Wireless Sensor Networks*, Morgan Kaufmann, San Francisco, 2004.